Preprint typeset in JHEP style. - PAPER VERSION

DTP/00/66,IPPP/00/05, MADPH-00-1197,hep-ph/0010212

Two-loop QCD corrections to the scattering of massless distinct quarks*

C. Anastasiou[a], **E. W. N. Glover**[a], **C. Oleari**[b] **and M. E. Tejeda-Yeomans**[a]

[a] *Department of Physics, University of Durham, Durham DH1 3LE, England*

[b] *Department of Physics, University of Wisconsin, 1150 University Avenue Madison WI 53706, U.S.A.*

E-mail: Ch.Anastasiou@durham.ac.uk, E.W.N.Glover@durham.ac.uk, Oleari@pheno.physics.wisc.edu, M.E.Tejeda-Yeomans@durham.ac.uk

ABSTRACT: We present the two-loop virtual QCD corrections to the scattering of distinct massless quarks, $q\bar{q} \to q'\bar{q}'$, in conventional dimensional regularisation. The structure of the infrared divergences agrees with that predicted by Catani while expressions for the finite remainder are given for each of the s-, t- and u-channels in terms of polylogarithms. The results presented here form a vital part of the next-to-next-to-leading order contribution to inclusive jet production in hadron colliders and will play a crucial role in improving the theoretical prediction for jet cross sections in hadron-hadron collisions.

KEYWORDS: QCD, Jets, LEP HERA and SLC Physics, NLO and NNLO Computations.

*Work supported in part by the UK Particle Physics and Astronomy Research Council and by the EU Fourth Framework Programme 'Training and Mobility of Researchers', Network 'Quantum Chromodynamics and the Deep Structure of Elementary Particles', contract FMRX-CT98-0194 (DG 12 - MIHT). C.A. acknowledges the financial support of the Greek government and M.E.T. acknowledges financial support from CONACyT and the CVCP. We thank the British Council and German Academic Exchange Service for support under ARC project 1050.

1. Introduction

In hadron-hadron collisions, the most basic hard process is parton-parton scattering to form a large transverse momentum jet. The single jet inclusive transverse energy distribution observed at the TEVATRON and CERN S$p\bar{p}$S shows good agreement with theoretical next-to-leading order $\mathcal{O}\left(\alpha_s^3\right)$ perturbative predictions over a wide range of jet transverse energies and tests the point-like nature of the partons down to distance scales of 10^{-17} m. However, data collected in Run I by the CDF collaboration at the TEVATRON indicated possible new physics at large transverse energy [1]. Data obtained by the D0 collaboration [2] was more consistent with next-to-leading order expectations. However, because of both theoretical and experimental uncertainties no definite conclusion could be drawn. The experimental situation may be clarified in the forthcoming Run II starting in 2001 where increased statistics and improved detectors may lead to a reduction in both the statistical and systematic errors.

The theoretical prediction may be improved by including the next-to-next-to-leading order perturbative predictions. This has the effect of (a) reducing the renormalisation scale dependence and (b) improving the matching of the parton level theoretical jet algorithm with the hadron level experimental jet algorithm because the jet structure can be modeled by the presence of a third parton. Varying the renormalisation scale up and down by a factor of two about the jet transverse energy leads to a 20% (10%) renormalisation scale uncertainty at leading order (next-to-leading order) for jets with $E_T \sim 100$ GeV. The improvement in accuracy expected at next-to-next-to-leading order can be estimated using the renormalisation group equations together with the known leading and next-to-leading order coefficients and is at the 1-2% level.

The full next-to-next-to-leading order prediction requires a knowledge of the two-loop $2 \to 2$ matrix elements as well as the contributions from the one-loop $2 \to 3$ and tree-level $2 \to 4$ processes. In the interesting large-transverse-energy region, $E_T \gg m_{\rm quark}$, the quark masses may be safely neglected and we therefore focus on the scattering of massless partons. For processes involving up, down and strange quarks, which together with processes involving gluons form the bulk of the cross section, this is certainly a reliable approximation. The contribution involving charm and bottom quarks is only a small part of the total since the parton densities for finding charm and bottom quarks inside the proton are relatively suppressed. We note that the existing next-to-leading order programs [3, 4] used to compare directly with the experimental jet data [1, 2] are based on massless parton-parton scattering. Helicity amplitudes for the one-loop $2 \to 3$ parton sub-processes $gg \to ggg$, $\bar{q}q \to ggg$, $\bar{q}q \to \bar{q}'q'g$, and processes related to these by crossing symmetry, have been computed in [5, 6, 7] respectively. The amplitudes for the six gluon $gg \to gggg$, four gluon-two quark $\bar{q}q \to gggg$, two gluon-four quark $\bar{q}q \to \bar{q}'q'gg$ and six quark $\bar{q}q \to \bar{q}'q'\bar{q}''q''$

$2 \to 4$ processes and the associated crossed processes computed at tree-level are also known and are available in [8, 9, 10, 11].

The calculation of the two-loop amplitudes for the massless $2 \to 2$ scattering processes

$$q + \bar{q} \to q' + \bar{q}' \tag{1.1}$$
$$q + \bar{q} \to q + \bar{q}, \tag{1.2}$$
$$q + \bar{q} \to g + g, \tag{1.3}$$
$$g + g \to g + g, \tag{1.4}$$

has proved more intractable due mainly to the difficulty of evaluating the planar and non-planar double box graphs. Recently however, analytic expressions for these basic scalar integrals for massless particle scattering have been provided by Smirnov [12] and by Tausk [13] as series in $\epsilon = (4 - D)/2$. Associated tensor integrals have also been solved in [14] and [15] so that generic two-loop massless $2 \to 2$ processes can in principle be expressed in terms of a basis set of known two-loop integrals. With the notable exception of the maximal helicity violating two loop amplitude for $gg \to gg$ which has recently been calculated by Bern, Dixon and Kosower [16][1], the two-loop matrix elements for the $2 \to 2$ QCD parton scattering processes are not known. It is the purpose of this paper to provide dimensionally regularised and renormalised analytic expressions at the two-loop level for process (1.1) together with the time-reversed and crossed processes

$$q + q' \to q + q',$$
$$q + \bar{q}' \to q + \bar{q}',$$
$$\bar{q} + \bar{q}' \to \bar{q} + \bar{q}'.$$

As is common in QCD calculations, we use the $\overline{\text{MS}}$ renormalisation scheme and conventional dimensional regularisation where all external particles are treated in D dimensions. We note that Bern, Dixon and Ghinculov [17] have recently completed the first full two-loop calculation of physical $2 \to 2$ scattering amplitudes, the QED processes $e^+e^- \to \mu^+\mu^-$ and $e^+e^- \to e^-e^+$. There is an overlap between their QED calculation and the QCD results presented here and we expect that the analytic expressions presented here will therefore provide a useful check of some of their results.

Our paper is structured as follows. In Section 2 we define our notation while a brief description of the methodology is given in Section 3. The results are collected in Section 4 where we provide analytic expressions for the interference of the two-loop and tree-level amplitudes as series expansions in ϵ. Catani has described the pole

[1]This amplitude vanishes at tree level and does therefore not contribute to $2 \to 2$ scattering at next-to-next-to-leading order $\mathcal{O}\left(\alpha_s^4\right)$.

structure of generic renormalised two-loop amplitudes [18] and we use his techniques to isolate the poles in the $\overline{\rm MS}$ scheme. We find that the pole structure expected in the $\overline{\rm MS}$ scheme on general grounds is indeed reproduced by direct evaluation of the Feynman diagrams. Ultimately these poles must be canceled by infrared singularities from tree level $2 \to 4$ and one-loop $2 \to 3$ processes. The finite remainder of the two-loop graphs form the main results of our paper and are given in Section 4. Our findings are summarized in Section 5.

2. Notation

For calculational convenience, we treat all particles as incoming so that

$$q(p_1) + \bar{q}(p_2) + q'(p_3) + \bar{q}'(p_4) \to 0 \tag{2.1}$$

where the light-like momentum assignments are in parentheses and satisfy

$$p_1^\mu + p_2^\mu + p_3^\mu + p_4^\mu = 0.$$

As stated above, we work in conventional dimensional regularisation treating all external states in D dimensions. We renormalise in the $\overline{\rm MS}$ scheme where the bare coupling α_0 is related to the running coupling $\alpha_s \equiv \alpha_s(\mu^2)$ at renormalisation scale μ via

$$\alpha_0\, S_\epsilon = \alpha_s \left[1 - \frac{\beta_0}{\epsilon}\left(\frac{\alpha_s}{2\pi}\right) + \left(\frac{\beta_0^2}{\epsilon^2} - \frac{\beta_1}{2\epsilon}\right)\left(\frac{\alpha_s}{2\pi}\right)^2 + \mathcal{O}\left(\alpha_s^3\right)\right]. \tag{2.2}$$

In this expression

$$S_\epsilon = (4\pi)^\epsilon e^{-\epsilon\gamma}, \qquad \gamma = 0.5772\ldots = \text{Euler constant} \tag{2.3}$$

is the typical phase-space volume factor in $D = 4 - 2\epsilon$ dimensions, and β_0, β_1 are the first two coefficients of the QCD beta function for N_F (massless) quark flavours

$$\beta_0 = \frac{11C_A - 4T_R\,N_F}{6}\ , \qquad \beta_1 = \frac{17C_A^2 - 10C_AT_R\,N_F - 6C_FT_R\,N_F}{6}\ . \tag{2.4}$$

For an $SU(N)$ gauge theory, where N is the number of colours

$$C_F = \left(\frac{N^2-1}{2N}\right), \qquad C_A = N, \qquad T_R = \frac{1}{2}. \tag{2.5}$$

The renormalised four point amplitude in the $\overline{\rm MS}$ scheme is thus

$$|\mathcal{M}\rangle = 4\pi\alpha_s\left[|\mathcal{M}^{(0)}\rangle + \left(\frac{\alpha_s}{2\pi}\right)|\mathcal{M}^{(1)}\rangle + \left(\frac{\alpha_s}{2\pi}\right)^2|\mathcal{M}^{(2)}\rangle + \mathcal{O}\left(\alpha_s^3\right)\right], \tag{2.6}$$

where the $|\mathcal{M}^{(i)}\rangle$ represents a colour space vector describing the i-loop amplitude. The dependence on both renormalisation scale μ and renormalisation scheme is implicit.

We denote the squared amplitude summed over spins and colours by

$$\langle \mathcal{M}|\mathcal{M}\rangle = \mathcal{A}(s,t,u), \tag{2.7}$$

where the Mandelstam variables are given by

$$s = (p_1+p_2)^2, \qquad t = (p_2+p_3)^2, \qquad u = (p_1+p_3)^2. \tag{2.8}$$

For the physical processes, the spin and colour averaged amplitudes are related to $\mathcal{A}$ by

$$\overline{\sum |\mathcal{M}(q+\bar{q}\to\bar{q}'+q')|^2} = \frac{1}{4N^2}\,\mathcal{A}(s,t,u) \tag{2.9}$$

$$\overline{\sum |\mathcal{M}(q+q'\to q+q')|^2} = \frac{1}{4N^2}\,\mathcal{A}(u,t,s) \tag{2.10}$$

$$\overline{\sum |\mathcal{M}(q+\bar{q}'\to\bar{q}'+q)|^2} = \frac{1}{4N^2}\,\mathcal{A}(t,s,u) \tag{2.11}$$

$$\overline{\sum |\mathcal{M}(\bar{q}+\bar{q}'\to\bar{q}+\bar{q}')|^2} = \frac{1}{4N^2}\,\mathcal{A}(u,t,s). \tag{2.12}$$

The summed and squared amplitude has the perturbative expansion

$$\mathcal{A}(s,t,u) = 16\pi^2\alpha_s^2\left[\mathcal{A}^4(s,t,u) + \left(\frac{\alpha_s}{2\pi}\right)\mathcal{A}^6(s,t,u) + \left(\frac{\alpha_s}{2\pi}\right)^2\mathcal{A}^8(s,t,u) + \mathcal{O}\left(\alpha_s^3\right)\right]. \tag{2.13}$$

In terms of the amplitudes

$$\mathcal{A}^4(s,t,u) = \langle\mathcal{M}^{(0)}|\mathcal{M}^{(0)}\rangle \equiv 2(N^2-1)\left(\frac{t^2+u^2}{s^2}-\epsilon\right), \tag{2.14}$$

$$\mathcal{A}^6(s,t,u) = \left(\langle\mathcal{M}^{(0)}|\mathcal{M}^{(1)}\rangle + \langle\mathcal{M}^{(1)}|\mathcal{M}^{(0)}\rangle\right), \tag{2.15}$$

$$\mathcal{A}^8(s,t,u) = \left(\langle\mathcal{M}^{(1)}|\mathcal{M}^{(1)}\rangle + \langle\mathcal{M}^{(0)}|\mathcal{M}^{(2)}\rangle + \langle\mathcal{M}^{(2)}|\mathcal{M}^{(0)}\rangle\right). \tag{2.16}$$

Expressions for $\mathcal{A}^6$ are given in Ref. [19] using dimensional regularisation to isolate the infrared and ultraviolet singularities.

Here we concentrate on the next-to-next-to-leading order contribution $\mathcal{A}^8$ and in particular the interference of the two-loop and tree graphs.

3. Method

Massless two-loop integrals for $2\to 2$ scattering can be described in terms of a basis set of scalar *master* integrals. The simpler massless master integrals comprise the trivial topologies of single scale integrals which can be written as products of Gamma functions:

Sunset(s) = 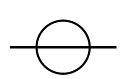 (s)

Glass(s) = 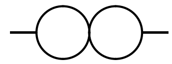 (s)

Tri(s) = 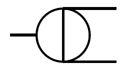 (s)

the less trivial non-planar triangle graph [20],

Xtri(s) = 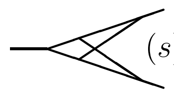 (s)

and two scale integrals that are related to the one-loop box graphs [21, 22],

Abox(s,t) = 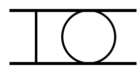 (s,t)

Cbox(s,t) = 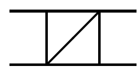 (s,t).

The planar double box [12] and non-planar double box [13]

Pbox$_1(s,t)$ = 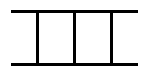 (s,t)

Xbox$_1(s,t)$ = 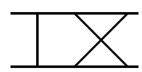 (s,t)

involve multiple Mellin-Barnes integrals and are much more complicated to evaluate as series expansions in ϵ. Expressions for these integrals valid through to $\mathcal{O}(\epsilon^0)$ are given in [12] and [13] respectively.

It turns out that for the two latter topologies, integrals involving loop momenta in the numerator cannot be entirely reduced in terms of the simpler integrals mentioned above and an additional master integral is required in each case. Reference [14] describes the procedure for reducing the tensor integrals down to a basis involving the planar box integral

Pbox$_2(s,t)$ = 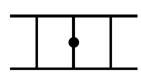 (s,t),

where the blob on the middle propagator represents an additional power of that propagator, and provides a series expansion for Pbox$_2$ to $\mathcal{O}(\epsilon^0)$. However, as was pointed out in [23], knowledge of Pbox$_1$ and Pbox$_2$ to $\mathcal{O}(\epsilon^0)$ is not sufficient to determine all tensor loop integrals to the same order. A better basis involves the tensor integral,

Pbox$_3(s,t)$ = 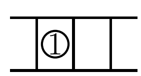 (s,t),

where ① represents the planar box integral with one irreducible numerator associated with the left loop. Symmetry of the integral ensures that,

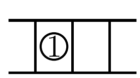 $(s,t) \equiv$ 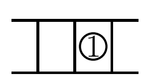 (s,t).

Series expansions for Pbox_3 are relatively compact and straightforward to obtain and are detailed in [24, 25]. Pbox_2 can therefore be eliminated in favor of Pbox_3. We note that this choice is not unique. Bern et al. [17] choose to use the Pbox_1 and Pbox_2 basis, but with the integrals evaluated in $D = 6 - 2\epsilon$ dimensions where they are both infrared and ultraviolet finite.

Similarly, the tensor reduction of the non-planar box integrals [15] also requires a second master integral,

$$\mathrm{Xbox}_2(s,t) =$$ 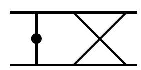 $$(s,t),$$

where the blob again denotes an additional power of the propagator. For the non-planar graphs there are no complications as in the planar case and all tensors to $\mathcal{O}(\epsilon^0)$ may be described in terms of the series expansions of Xbox_1 and Xbox_2 through to $\mathcal{O}(\epsilon^0)$ [13, 15].

In general tensor integrals are associated with scalar integrals in higher dimension and with higher powers of propagators. This connection can straightforwardly be achieved using the Schwinger parameter form of the integral and is detailed in [22] where explicit expressions for generic two-loop integrals with up to four powers of loop momenta in the numerator are given[2]. Systematic application of the integration-by-parts (IBP) identities [27] and Lorentz invariance (LI) identities [28] is sufficient to reduce these higher-dimension, higher-power integrals to master integrals in $D = 4 - 2\epsilon$. Some topologies that occur in Feynman diagrams such as the pentabox [22] are immediately simplified using the IBP identities and collapse to combinations of master integrals. However, the tensor integrals directly associated with the master integrals usually require more care. Explicit identities relevant for the tensor integrals of the Abox and Cbox topologies are given in [22], for Pbox_1 and Pbox_2 integrals in [14] while those for the Xtri, Xbox_1 and Xbox_2 integrals are detailed in [15]. Using these identities, we have constructed MAPLE and FORM programs to rewrite two-loop tensor integrals for massless $2 \to 2$ scattering directly in terms of the basis set of master integrals.

The one-loop integrals are much better known. There are only two master integrals, the scalar bubble graph,

$$\mathrm{Bub}(s) =$$ 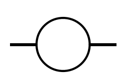 $$(s) \quad ,$$

and the one-loop scalar box graph,

$$\mathrm{Box}(s,t) =$$ 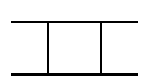 $$(s,t).$$

[2] A method to reduce tensor integrals constructing differential operators that change the powers of the propagators as well as the dimension of the integral was presented in Ref. [26].

We treat the tensor integrals in the same way as the two-loop integrals: shifting both dimension and powers of propagators and then using IBP to rewrite the integrals as combinations of Bub and Box. We note that this is not a unique choice for the master integrals. The one-loop bubble graph is proportional to the one-loop triangle graph with one off-shell leg. Another common choice is to replace the one-loop box in $D = 4 - 2\epsilon$ by the finite one-loop box in $D = 6 - 2\epsilon$, Box^6.

The general procedure for computing the amplitudes is therefore as follows. First the two-loop Feynman diagrams are generated using `QGRAF` [29]. We then project by tree level, perform the summation over colours and spins and trace over the Dirac matrices in D dimensions using conventional dimensional regularisation. It is then straightforward to identify the scalar and tensor integrals present and replace them with combinations of master integrals using the tensor reduction of two-loop integrals described in [14, 15, 22] based on integration-by-parts [27] and Lorentz invariance [28] identities. The final result is a combination of master integrals in $D = 4 - 2\epsilon$ which can be substituted for the expansions in ϵ given in [12, 13, 14, 15, 21, 22, 24, 25].

4. Results

In this section, we give explicit formulae for the ϵ-expansion of the two-loop contribution to the next-to-next-to-leading order term $\mathcal{A}^8(s,t,u)$. To distinguish between the genuine two-loop contribution $\langle \mathcal{M}^{(0)} | \mathcal{M}^{(2)} \rangle + \langle \mathcal{M}^{(2)} | \mathcal{M}^{(0)} \rangle$ and the squared one-loop part $\langle \mathcal{M}^{(1)} | \mathcal{M}^{(1)} \rangle$, we decompose $\mathcal{A}^8$ as

$$\mathcal{A}^8 = \mathcal{A}^{8\ (2\times 0)} + \mathcal{A}^{8\ (1\times 1)}. \tag{4.1}$$

The one-loop-square contribution $\mathcal{A}^{8\ (1\times 1)}$ is vital in determining $\mathcal{A}^8$ but is relatively straightforward to obtain. For the remainder of this paper we concentrate on the technically more complicated two-loop contribution $\mathcal{A}^{8\ (2\times 0)}$.

We divide the two-loop contributions into two classes: those that multiply poles in the dimensional regularisation parameter ϵ and those that are finite as $\epsilon \to 0$

$$\mathcal{A}^{8\ (2\times 0)}(s,t,u) = \mathcal{P}oles + \mathcal{F}inite. \tag{4.2}$$

$\mathcal{P}oles$ contains both infrared singularities and ultraviolet divergences. The latter are removed by renormalisation, while the former must be analytically canceled by the infrared singularities occurring in radiative processes of the same order. The structure of these infrared divergences has been widely studied and, as has been demonstrated by Catani [18], can be largely predicted.

4.1 Infrared pole structure

In the notation of Section 2, the universal infrared divergences present in a one-loop amplitude are given by the factorization formulae

$$|\mathcal{M}^{(1)}\rangle = \boldsymbol{I}^{(1)}(\epsilon)\, |\mathcal{M}^{(0)}\rangle + |\mathcal{M}^{(1)\,\text{fin}}\rangle, \tag{4.3}$$

where $|\mathcal{M}^{(1)\,\mathrm{fin}}\rangle$ is finite as $\epsilon \to 0$ and the singular dependence is determined by the colour-charge operator $\boldsymbol{I}^{(1)}(\epsilon)$ that acts on the tree-level colour vector $|\mathcal{M}^{(0)}\rangle$. For the n parton process we sum over all possible colour antennae with colour operators $\boldsymbol{T}_i \cdot \boldsymbol{T}_j$ acting on the state $|\mathcal{M}^{(0)}\rangle$ to obtain

$$\boldsymbol{I}^{(1)}(\epsilon) = \frac{1}{2}\frac{e^{\epsilon\gamma}}{\Gamma(1-\epsilon)}\sum_{i=1}^{n}\sum_{i\neq j}^{n}\boldsymbol{T}_i \cdot \boldsymbol{T}_j \left(\frac{1}{\epsilon^2}+\frac{\gamma_i}{\epsilon}\right)\left(\frac{\mu^2 e^{-i\lambda_{ij}\pi}}{2p_i.p_j}\right)^{\epsilon} \tag{4.4}$$

and where $\lambda_{ij} = -1$ if i and j are both incoming or outgoing partons and $\lambda_{ij} = 0$ otherwise and the constants γ_i are given by

$$\gamma_q = \gamma_{\bar{q}} = \frac{3}{2}, \qquad \gamma_g = \frac{\beta_0}{C_A}. \tag{4.5}$$

Similarly at the two-loop level there is a factorisation of the infrared singularities

$$|\mathcal{M}^{(2)}\rangle = \boldsymbol{I}^{(1)}(\epsilon)\,|\mathcal{M}^{(1)}\rangle + \boldsymbol{I}^{(2)}(\epsilon)\,|\mathcal{M}^{(0)}\rangle + |\mathcal{M}^{(2)\,\mathrm{fin}}\rangle \tag{4.6}$$

where now

$$\boldsymbol{I}^{(2)}(\epsilon) = -\frac{1}{2}\boldsymbol{I}^{(1)}(\epsilon)\left(\boldsymbol{I}^{(1)}(\epsilon)+\frac{2\beta_0}{\epsilon}\right) + e^{-\epsilon\gamma}\frac{\Gamma(1-2\epsilon)}{\Gamma(1-\epsilon)}\left(\frac{\beta_0}{\epsilon}+K\right)\boldsymbol{I}^{(1)}(2\epsilon) + \boldsymbol{H}^{(2)}(\epsilon) \tag{4.7}$$

where the constant K is

$$K = \left(\frac{67}{18}-\frac{\pi^2}{6}\right)C_A - \frac{10}{9}T_R\,N_F. \tag{4.8}$$

The function $\boldsymbol{H}^{(2)}$ contains only single poles and is process dependent. For the case of the quark form factor (in the $\overline{\mathrm{MS}}$ scheme) it is given by

$$\boldsymbol{H}^{(2)}(\epsilon) = \frac{1}{4\epsilon}\frac{e^{\epsilon\gamma}}{\Gamma(1-\epsilon)}\left(\frac{\mu^2 e^{-i\lambda_{12}\pi}}{2p_1.p_2}\right)^{2\epsilon} H^{(2)}, \tag{4.9}$$

with

$$H^{(2)} = \left[\frac{1}{4}\gamma_{(1)} + 3C_F K + \frac{5}{2}\zeta_2\beta_0 C_F - \frac{28}{9}\beta_0 C_F - \left(\frac{16}{9}-7\zeta_3\right)C_F C_A\right] \tag{4.10}$$

where ζ_n is the Riemann Zeta function, $\zeta_2 = \pi^2/6$, $\zeta_3 = 1.202056\ldots$ and

$$\gamma_{(1)} = (-3+24\zeta_2-48\zeta_3)\,C_F^2 + \left(-\frac{17}{3}-\frac{88}{3}\zeta_2+24\zeta_3\right)C_F C_A + \left(\frac{4}{3}+\frac{32}{3}\zeta_2\right)C_F T_R\,N_F. \tag{4.11}$$

We expect that in the four-quark two loop amplitude, we might obtain contributions from $\boldsymbol{H}^{(2)}$ for each of the six colour antennae.

Applying the formalism to the case at hand, we find that the pole structure of the two-loop amplitude interfered with tree level has the following structure

$$\begin{aligned}\mathcal{P}oles = 2\,\mathrm{Re}\Bigg[& \frac{1}{2}\langle\mathcal{M}^{(0)}|\boldsymbol{I}^{(1)}(\epsilon)\boldsymbol{I}^{(1)}(\epsilon)|\mathcal{M}^{(0)}\rangle - \frac{\beta_0}{\epsilon}\langle\mathcal{M}^{(0)}|\boldsymbol{I}^{(1)}(\epsilon)|\mathcal{M}^{(0)}\rangle \\ & + \langle\mathcal{M}^{(0)}|\boldsymbol{I}^{(1)}(\epsilon)|\mathcal{M}^{(1)\,\mathrm{fin}}\rangle \\ & + e^{-\epsilon\gamma}\frac{\Gamma(1-2\epsilon)}{\Gamma(1-\epsilon)}\left(\frac{\beta_0}{\epsilon}+K\right)\langle\mathcal{M}^{(0)}|\boldsymbol{I}^{(1)}(2\epsilon)|\mathcal{M}^{(0)}\rangle \\ & + \langle\mathcal{M}^{(0)}|\boldsymbol{H}^{(2)}(\epsilon)|\mathcal{M}^{(0)}\rangle\Bigg]. \end{aligned} \tag{4.12}$$

The colour algebra is straightforward and we find

$$\begin{aligned}&\langle\mathcal{M}^{(0)}|\boldsymbol{I}^{(1)}(\epsilon)|\mathcal{M}^{(0)}\rangle = \langle\mathcal{M}^{(0)}|\mathcal{M}^{(0)}\rangle \\ &\times\frac{e^{\epsilon\gamma}}{\Gamma(1-\epsilon)}\left(\frac{1}{\epsilon^2}+\frac{3}{2\epsilon}\right)\left[\frac{1}{N}\left(-\frac{\mu^2}{s}\right)^{\epsilon} - \frac{2}{N}\left(-\frac{\mu^2}{u}\right)^{\epsilon} - \frac{N^2-2}{N}\left(-\frac{\mu^2}{t}\right)^{\epsilon}\right]\end{aligned} \tag{4.13}$$

$$\begin{aligned}&\langle\mathcal{M}^{(0)}|\boldsymbol{I}^{(1)}(\epsilon)\boldsymbol{I}^{(1)}(\epsilon)|\mathcal{M}^{(0)}\rangle = \langle\mathcal{M}^{(0)}|\mathcal{M}^{(0)}\rangle \\ &\times\frac{e^{2\epsilon\gamma}}{\Gamma(1-\epsilon)^2}\left(\frac{1}{\epsilon^2}+\frac{3}{2\epsilon}\right)^2\left[\frac{N^4-3N^2+3}{N^2}\left(-\frac{\mu^2}{t}\right)^{2\epsilon} + \frac{N^2+3}{N^2}\left(-\frac{\mu^2}{u}\right)^{2\epsilon}\right. \\ &\qquad - 2\frac{N^2-2}{N^2}\left(-\frac{\mu^2}{s}\right)^{\epsilon}\left(-\frac{\mu^2}{t}\right)^{\epsilon} + 2\frac{N^2-3}{N^2}\left(-\frac{\mu^2}{t}\right)^{\epsilon}\left(-\frac{\mu^2}{u}\right)^{\epsilon} \\ &\qquad\left. - \frac{4}{N^2}\left(-\frac{\mu^2}{s}\right)^{\epsilon}\left(-\frac{\mu^2}{u}\right)^{\epsilon} + \frac{1}{N^2}\left(-\frac{\mu^2}{s}\right)^{2\epsilon}\right]\end{aligned} \tag{4.14}$$

$$\begin{aligned}&\langle\mathcal{M}^{(0)}|\boldsymbol{I}^{(1)}(\epsilon)|\mathcal{M}^{(1)\,\mathrm{fin}}\rangle = \frac{e^{\epsilon\gamma}}{\Gamma(1-\epsilon)}\left(\frac{1}{\epsilon^2}+\frac{3}{2\epsilon}\right) \\ &\times\left\{\left[\frac{1}{N}\left(-\frac{\mu^2}{s}\right)^{\epsilon} - \frac{2}{N}\left(-\frac{\mu^2}{u}\right)^{\epsilon} - \frac{N^2-2}{N}\left(-\frac{\mu^2}{t}\right)^{\epsilon}\right]\mathcal{F}_1(s,t,u)\right. \\ &\qquad\left. + \left[\frac{1}{N}\left(-\frac{\mu^2}{u}\right)^{\epsilon} - \frac{1}{N}\left(-\frac{\mu^2}{t}\right)^{\epsilon}\right](N^2-1)\,\mathcal{F}_2(s,t,u)\right\}\end{aligned} \tag{4.15}$$

and

$$\begin{aligned}&\langle\mathcal{M}^{(0)}|\boldsymbol{H}^{(2)}(\epsilon)|\mathcal{M}^{(0)}\rangle = \langle\mathcal{M}^{(0)}|\mathcal{M}^{(0)}\rangle \\ &\qquad\times\frac{e^{\epsilon\gamma}}{2\,\epsilon\,\Gamma(1-\epsilon)}H^{(2)}\left[\left(-\frac{\mu^2}{s}\right)^{2\epsilon} + \left(-\frac{\mu^2}{t}\right)^{2\epsilon} - \left(-\frac{\mu^2}{u}\right)^{2\epsilon}\right],\end{aligned} \tag{4.16}$$

where the square bracket in Eq. (4.16) is a guess simply motivated by summing over the antennae present in the quark-quark scattering process and on dimensional grounds. Different choices only affect the finite remainder.

The functions $\mathcal{F}_1$ and $\mathcal{F}_2$ appearing in Eq. (4.15) are finite functions and are obtained from projection of $\boldsymbol{I}^{(1)}$ onto the one-loop amplitude. We find

$$\begin{aligned}
\mathcal{F}_1(s,t,u) = &\frac{N^2-1}{2N}\left[\left(N^2-2\right)f(s,t,u)+2f(s,u,t)\right] \\
&-\frac{1}{2\epsilon(3-2\epsilon)}\left[\frac{N^2-1}{N}\left(6-7\epsilon-2\epsilon^2\right)-\frac{1}{N}\left(10\epsilon^2-4\epsilon^3\right)\right]\mathrm{Bub}(s)\langle\mathcal{M}^{(0)}|\mathcal{M}^{(0)}\rangle \\
&-\frac{e^{\epsilon\gamma}}{\Gamma(1-\epsilon)}\left(\frac{1}{\epsilon^2}+\frac{3}{2\epsilon}\right)\left[\frac{1}{N}\left(-\frac{\mu^2}{s}\right)^{\epsilon}-\frac{2}{N}\left(-\frac{\mu^2}{u}\right)^{\epsilon}-\frac{N^2-2}{N}\left(-\frac{\mu^2}{t}\right)^{\epsilon}\right]\langle\mathcal{M}^{(0)}|\mathcal{M}^{(0)}\rangle \\
&-\beta_0\left[\frac{1}{\epsilon}-\frac{3(1-\epsilon)}{(3-2\epsilon)}\mathrm{Bub}(s)\right]\langle\mathcal{M}^{(0)}|\mathcal{M}^{(0)}\rangle \qquad (4.17)
\end{aligned}$$

$$\begin{aligned}
\mathcal{F}_2(s,t,u) = &\frac{N^2-1}{2N}\left[f(s,t,u)-f(s,u,t)\right] \\
&-\frac{e^{\epsilon\gamma}}{\Gamma(1-\epsilon)}\left(\frac{1}{\epsilon^2}+\frac{3}{2\epsilon}\right)\left[\frac{1}{N}\left(-\frac{\mu^2}{u}\right)^{\epsilon}-\frac{1}{N}\left(-\frac{\mu^2}{t}\right)^{\epsilon}\right]\langle\mathcal{M}^{(0)}|\mathcal{M}^{(0)}\rangle \qquad (4.18)
\end{aligned}$$

where the function $f(s,t,u)$ is written in terms of the one-loop box graph in $D = 6-2\epsilon$ and the one-loop bubble graph in $D = 4-2\epsilon$

$$\begin{aligned}
f(s,t,u) = &\frac{4(u^2+t^2)-2\epsilon(3ut+6t^2+5u^2)-\epsilon^2 s(7t+5u)}{s^2}\left[\frac{\mathrm{Bub}(s)-\mathrm{Bub}(t)}{\epsilon}\right] \\
&+u\,(1-2\,\epsilon)\frac{6t^2+2u^2-3\epsilon s^2}{s^2}\,\mathrm{Box}^6(s,t). \qquad (4.19)
\end{aligned}$$

These expressions are valid in all kinematic regions. However, to evaluate the pole structure in a particular region, they must be expanded as a series in ϵ. We note that in Eq. (4.12), these functions are multiplied by poles in ϵ and must therefore be expanded through to $\mathcal{O}\left(\epsilon^2\right)$. In the physical region $u<0$, $t<0$, $\mathrm{Box}^6(u,t)$ has no imaginary part and is given by [17]

$$\begin{aligned}
\mathrm{Box}^6(u,t) = &\frac{e^{\epsilon\gamma}\Gamma\left(1+\epsilon\right)\Gamma\left(1-\epsilon\right)^2}{2s\Gamma\left(1-2\epsilon\right)\left(1-2\epsilon\right)}\left(\frac{\mu^2}{s}\right)^{\epsilon}\left[\frac{1}{2}\left((L_x-L_y)^2+\pi^2\right)\right. \\
&+2\epsilon\left(\mathrm{Li}_3(x)-L_x\mathrm{Li}_2(x)-\frac{1}{3}L_x^3-\frac{\pi^2}{2}L_x\right) \\
&-2\epsilon^2\left(\mathrm{Li}_4(x)+L_y\mathrm{Li}_3(x)-\frac{1}{2}L_x^2\mathrm{Li}_2(x)-\frac{1}{8}L_x^4-\frac{1}{6}L_x^3L_y+\frac{1}{4}L_x^2L_y^2\right. \\
&\left.\left.-\frac{\pi^2}{4}L_x^2-\frac{\pi^2}{3}L_xL_y-\frac{\pi^4}{45}\right)+(u\leftrightarrow t)\right]+\mathcal{O}\left(\epsilon^3\right), \qquad (4.20)
\end{aligned}$$

where $x=-t/s$, $L_x=\log(x)$ and $L_y=\log(1-x)$ and the polylogarithms $\mathrm{Li}_n(z)$ are defined by

$$\mathrm{Li}_n(z) = \int_0^z \frac{dt}{t}\mathrm{Li}_{n-1}(t) \qquad \text{for } n=2,3,4 \qquad (4.21)$$

$$\mathrm{Li}_2(z) = -\int_0^z \frac{dt}{t}\log(1-t). \qquad (4.22)$$

Analytic continuation to other kinematic regions is obtained using the inversion formulae for the arguments of the polylogarithms (see for example [22]) when $x > 1$

$$\begin{aligned}
\mathrm{Li}_2(x+i0) &= -\mathrm{Li}_2\left(\frac{1}{x}\right) - \frac{1}{2}\log^2(x) + \frac{\pi^2}{3} + i\pi\log(x) \\
\mathrm{Li}_3(x+i0) &= \mathrm{Li}_3\left(\frac{1}{x}\right) - \frac{1}{6}\log^3(x) + \frac{\pi^2}{3}\log(x) + \frac{i\pi}{2}\log^2(x) \\
\mathrm{Li}_4(x+i0) &= -\mathrm{Li}_4\left(\frac{1}{x}\right) - \frac{1}{24}\log^4(x) + \frac{\pi^2}{6}\log^2(x) + \frac{\pi^4}{45} + \frac{i\pi}{6}\log^3(x). \quad (4.23)
\end{aligned}$$

Finally, the one-loop bubble integral in $D = 4 - 2\epsilon$ dimensions is given by

$$\mathrm{Bub}(s) = \frac{e^{\epsilon\gamma}\Gamma(1+\epsilon)\Gamma(1-\epsilon)^2}{\Gamma(2-2\epsilon)\,\epsilon}\left(-\frac{\mu^2}{s}\right)^{\epsilon}. \quad (4.24)$$

Our explicit Feynman diagram reproduces the anticipated pole structure exactly and provides a very stringent check on the calculation. We therefore construct the finite remainder by subtracting Eq. (4.12) from the full result.

4.2 Finite contributions

In this subsection, we give explicit expressions for the finite two-loop contribution to $\mathcal{A}^8$, $\mathcal{F}inite$, which is given by

$$\mathcal{F}inite = 2\,\mathrm{Re}\langle\mathcal{M}^{(0)}|\mathcal{M}^{(2)\,\mathrm{fin}}\rangle. \quad (4.25)$$

For high energy hadron-hadron collisions, we probe all parton-parton scattering processes simultaneously. We therefore need to be able to evaluate the finite parts in the s-, t- and u-channels corresponding to the processes

$$\begin{aligned}
q + \bar{q} &\to \bar{q}' + q' \\
q + \bar{q}' &\to \bar{q}' + q \\
q + q' &\to q + q',
\end{aligned}$$

respectively. In principle, the analytic expressions for different channels are related by crossing symmetry. However, the Xbox has cuts in all three channels yielding complex parts in all physical regions. The analytic continuation is therefore rather involved and prone to error. We therefore choose to give expressions describing $\mathcal{A}^8(s,t,u)$, $\mathcal{A}^8(t,s,u)$ and $\mathcal{A}^8(u,t,s)$ which are directly valid in the physical region, $s > 0$ and $u, t < 0$, and are given in terms of logarithms and polylogarithms that have no imaginary parts.

In general the expansions of the two-loop master integrals [12, 13, 14, 15, 22, 24, 25] contain the generalised polylogarithms of Nielsen

$$\mathrm{S}_{n,p}(x) = \frac{(-1)^{n+p-1}}{(n-1)!\,p!}\int_0^1 dt\,\frac{\log^{n-1}(t)\log^p(1-xt)}{t}, \qquad n,p \geq 1, \quad x \leq 1 \quad (4.26)$$

where the level is $n+p$. Keeping terms up to $\mathcal{O}(\epsilon)$ corresponds to probing level 4 so that only polylogarithms with $n+p \leq 4$ occur. For $p=1$ we find the usual polylogarithms

$$\mathrm{S}_{n-1,1}(z) \equiv \mathrm{Li}_n(z). \tag{4.27}$$

A basis set of 6 polylogarithms (one with $n+p=2$, two with $n+p=3$ and three with $n+p=4$ is sufficient to describe a function of level 4. At level 4, we choose to eliminate the S_{22}, S_{13} and S_{12} functions using the standard polylogarithm identities [30] and retain the polylogarithms with arguments x, $1-x$ and $(x-1)/x$, where

$$x = -\frac{t}{s}, \qquad y = -\frac{u}{s} = 1-x, \qquad -\frac{u}{t} = \frac{x-1}{x}. \tag{4.28}$$

For convenience, we also introduce the following logarithms

$$L_x = \log\left(\frac{-t}{s}\right), \qquad L_y = \log\left(\frac{-u}{s}\right), \qquad L_s = \log\left(\frac{s}{\mu^2}\right) \tag{4.29}$$

where μ is the renormalisation scale. The common choice $\mu^2 = s$ corresponds to setting $L_s = 0$.

For each channel, we choose to present our results by grouping terms according to the power of the number of colours N and the number of light quarks N_F so that in channel c

$$\mathcal{F}inite_c = 2\Big(N^2-1\Big)\left(N^2 A_c + B_c + \frac{1}{N^2}C_c + N\,N_F D_c + \frac{N_F}{N}E_c + N_F^2 F_c\right). \tag{4.30}$$

4.2.1 The s-channel process $q\bar{q} \to \bar{q}'q'$

We first give expressions for the s-channel annihilation process, $q\bar{q} \to \bar{q}'q'$. We find that

$$\begin{aligned}
A_s = \Bigg[& 2\,\mathrm{Li}_4(x) + \left(-2\,L_x - \frac{11}{3}\right)\mathrm{Li}_3(x) + \left(L_x^2 + \frac{11}{3}\,L_x - \frac{2}{3}\,\pi^2\right)\mathrm{Li}_2(x) \\
& + \frac{121}{18}\,L_s^2 + \left(-\frac{11}{3}\,L_x^2 + 11\,L_x - \frac{296}{27}\right)L_s + \frac{1}{6}\,L_x^4 + \left(\frac{1}{3}\,L_y - \frac{49}{18}\right)L_x^3 \\
& + \left(\frac{11}{6}\,L_y - \frac{5}{6}\,\pi^2 + \frac{197}{18}\right)L_x^2 + \left(-\frac{2}{3}\,L_y\,\pi^2 - \frac{47}{18}\,\pi^2 + 6\,\zeta_3 - \frac{95}{24}\right)L_x \\
& + \left(\frac{11}{24}\,\pi^2 - 7\,\zeta_3 - \frac{409}{216}\right)L_y + \frac{113}{720}\,\pi^4 - \frac{7}{6}\,\pi^2 + \frac{197}{36}\,\zeta_3 + \frac{23213}{2592}\Bigg]\left[\frac{t^2+u^2}{s^2}\right] \\
& + \Bigg[-3\,\mathrm{Li}_4(y) + 6\,\mathrm{Li}_4(x) - 3\,\mathrm{Li}_4\left(\frac{x-1}{x}\right) + \left(-2\,L_x - \frac{7}{2}\right)\mathrm{Li}_3(x) \\
& + 3\,L_x\,\mathrm{Li}_3(y) + \left(\frac{1}{2}\,L_x^2 + \frac{7}{2}\,L_x + \frac{1}{2}\,\pi^2\right)\mathrm{Li}_2(x) + \left(-\frac{11}{6}\,L_x^2 + \frac{11}{6}\,L_x\right)L_s \\
& + \left(\frac{1}{2}\,L_y\,\pi^2 - \frac{13}{9}\,\pi^2 - \zeta_3 - \frac{32}{9}\right)L_x + \left(\frac{7}{4}\,L_y - \frac{3}{4}\,\pi^2 + \frac{44}{9}\right)L_x^2
\end{aligned}$$

$$+\left(\frac{1}{2}\,L_y-\frac{49}{36}\right)L_x^3-\frac{7}{120}\,\pi^4+\frac{47}{36}\,\pi^2+2\,\zeta_3\Bigg]\left[\frac{t^2-u^2}{s^2}\right]+\left[3\,L_x^2\right]\frac{t^3}{s^2u}$$

$$+3\,\mathrm{Li}_4(y)-3\,\mathrm{Li}_4(x)+3\,\mathrm{Li}_4\!\left(\frac{x-1}{x}\right)-3\,L_x\,\mathrm{Li}_3(y)-\frac{5}{2}\,\mathrm{Li}_3(x)$$

$$+\left(\frac{5}{2}\,L_x-\frac{1}{2}\,\pi^2\right)\mathrm{Li}_2(x)-\frac{11}{6}\,L_x\,L_s+\frac{1}{8}\,L_x^4+\left(-\frac{1}{2}\,L_y+\frac{1}{3}\right)L_x^3$$

$$+\left(\frac{5}{4}\,L_y+\frac{1}{4}\,\pi^2+\frac{1}{6}\right)L_x^2+\left(-\frac{1}{2}\,L_y\,\pi^2-\frac{7}{6}\,\pi^2+3\,\zeta_3+\frac{32}{9}\right)L_x$$

$$+\frac{1}{40}\,\pi^4-\frac{11}{36}\,\pi^2+4\,\zeta_3 \qquad (4.31)$$

$$B_s=\Bigg[-6\,\mathrm{Li}_4(x)-\frac{22}{3}\,\mathrm{Li}_3(y)+\left(-3\,L_x^2-\frac{22}{3}\,L_x-\frac{22}{3}\,L_y+2\,\pi^2\right)\mathrm{Li}_2(x)$$

$$+\left(6\,L_x+\frac{22}{3}\right)\mathrm{Li}_3(x)+\left(\frac{22}{3}\,L_x^2-22\,L_x-\frac{22}{3}\,L_y^2+22\,L_y-\frac{88}{3}\right)L_s$$

$$-\frac{1}{2}\,L_x^4+\left(-L_y+\frac{125}{18}\right)L_x^3+\left(\frac{1}{2}\,L_y^2-\frac{31}{6}\,L_y+3\,\pi^2-\frac{743}{36}\right)L_x^2$$

$$+\left(-\frac{31}{6}\,L_y^2+\left(-\frac{4}{3}\,\pi^2+\frac{9}{2}\right)L_y+\frac{307}{72}\,\pi^2+\zeta_3-\frac{49}{27}\right)L_x$$

$$+\frac{1}{4}\,L_y^4-\frac{71}{18}\,L_y^3+\left(-\frac{2}{3}\,\pi^2+\frac{689}{36}\right)L_y^2+\left(-\frac{73}{24}\,\pi^2-\zeta_3-\frac{275}{27}\right)L_y$$

$$+\frac{79}{720}\,\pi^4-\frac{55}{72}\,\pi^2-\frac{443}{36}\,\zeta_3+\frac{30659}{648}\Bigg]\left[\frac{t^2+u^2}{s^2}\right]$$

$$+\Bigg[-12\,\mathrm{Li}_4(y)+3\,\mathrm{Li}_4(x)-8\,\mathrm{Li}_4\!\left(\frac{x-1}{x}\right)+\left(2\,L_y+8\right)\mathrm{Li}_3(y)$$

$$+\left(-\frac{3}{2}\,L_x^2+\left(-8\,L_y-\frac{11}{2}\right)L_x+8\,L_y-\frac{4}{3}\,\pi^2\right)\mathrm{Li}_2(x)-12\,L_y\,L_x\,\mathrm{Li}_2(y)$$

$$+\left(4\,L_x-12\,L_y+\frac{11}{2}\right)\mathrm{Li}_3(x)+\left(\frac{11}{3}\,L_x^2-\frac{11}{3}\,L_x+\frac{11}{3}\,L_y^2-\frac{11}{3}\,L_y\right)L_s$$

$$-\frac{17}{24}\,L_x^4+\left(L_y+\frac{131}{36}\right)L_x^3+\left(-\frac{25}{2}\,L_y^2-\frac{15}{4}\,L_y+\frac{13}{12}\,\pi^2-\frac{289}{36}\right)L_x^2$$

$$+\left(\frac{1}{3}\,L_y^3+5\,L_y^2+\frac{5}{3}\,L_y\,\pi^2+\frac{89}{36}\,\pi^2+\frac{37}{9}\right)L_x-\frac{1}{6}\,L_y^4+\frac{17}{9}\,L_y^3$$

$$+\left(\frac{7}{12}\,\pi^2-\frac{361}{36}\right)L_y^2+\left(\frac{59}{36}\,\pi^2+6\,\zeta_3+\frac{64}{9}\right)L_y-\frac{1}{20}\,\pi^4-\frac{44}{9}\,\pi^2-9\,\zeta_3\Bigg]\left[\frac{t^2-u^2}{s^2}\right]$$

$$\left[-7\,L_x^2\right]\frac{t^3}{s^2u}+\left[5\,L_y^2\right]\frac{u^3}{s^2t}-12\,\mathrm{Li}_4(y)+12\,\mathrm{Li}_4(x)-12\,\mathrm{Li}_4\!\left(\frac{x-1}{x}\right)$$

$$+\left(6\,L_x-6\right)\mathrm{Li}_3(y)+\left(-6\,L_y+\frac{9}{2}\right)\mathrm{Li}_3(x)-6\,L_y\,L_x\,\mathrm{Li}_2(y)$$

$$
\begin{aligned}
&+\Bigg(\Big(-6\,L_y-\frac{9}{2}\Big)\,L_x-6\,L_y+2\,\pi^2\Bigg)\,\mathrm{Li}_2(x)+\Big(\frac{11}{3}\,L_x-\frac{11}{3}\,L_y\Big)\,L_s\\
&-\frac{1}{2}\,L_x^4+\Big(2\,L_y-\frac{5}{6}\Big)\,L_x^3+\Big(-\frac{15}{2}\,L_y^2-2\,L_y-\pi^2+\frac{17}{12}\Big)\,L_x^2\\
&+\Bigg(-\frac{11}{4}\,L_y^2+\Big(3\,\pi^2+\frac{1}{2}\Big)\,L_y+\frac{25}{12}\,\pi^2-6\,\zeta_3-\frac{37}{9}\Bigg)\,L_x+\frac{1}{4}\,L_y^3\\
&+\frac{7}{12}\,L_y^2+\Big(-\frac{5}{4}\,\pi^2+6\,\zeta_3+\frac{64}{9}\Big)\,L_y-\frac{17}{60}\,\pi^4-\frac{2}{3}\,\pi^2+5\,\zeta_3
\end{aligned}
\tag{4.32}
$$

$$
\begin{aligned}
C_s=&\Bigg[16\,\mathrm{Li}_4(y)+8\,\mathrm{Li}_4(x)-16\,L_y\,\mathrm{Li}_3(y)-8\,L_x\,\mathrm{Li}_3(x)+\Big(4\,L_x^2+\frac{8}{3}\,\pi^2\Big)\,\mathrm{Li}_2(x)\\
&+8\,L_y^2\,\mathrm{Li}_2(y)+\frac{5}{12}\,L_x^4+\Big(\frac{4}{3}\,L_y-\frac{9}{2}\Big)\,L_x^3+\Big(-\frac{3}{2}\,L_y^2+\frac{9}{2}\,L_y-\frac{11}{3}\,\pi^2+\frac{1}{4}\Big)\,L_x^2\\
&+\Bigg(\frac{8}{3}\,L_y^3+\frac{9}{2}\,L_y^2+\Big(\frac{22}{3}\,\pi^2-\frac{27}{2}\Big)\,L_y+\frac{1}{2}\,\pi^2-6\,\zeta_3+\frac{189}{8}\Bigg)\,L_x\\
&+\frac{1}{12}\,L_y^4-\frac{9}{2}\,L_y^3+\Big(-\frac{7}{3}\,\pi^2+\frac{65}{4}\Big)\,L_y^2+\Big(-\frac{1}{2}\,\pi^2+6\,\zeta_3-\frac{189}{8}\Big)\,L_y\\
&-\frac{49}{60}\,\pi^4+\frac{29}{24}\,\pi^2-\frac{15}{2}\,\zeta_3+\frac{511}{32}\Bigg]\,\Bigg[\frac{t^2+u^2}{s^2}\Bigg]\\
&+\Bigg[12\,\mathrm{Li}_4(y)-24\,\mathrm{Li}_4(x)+24\,\mathrm{Li}_4\Big(\frac{x-1}{x}\Big)+\Big(-18\,L_x+10\,L_y-2\Big)\,\mathrm{Li}_3(y)\\
&+\Big(-2\,L_x+18\,L_y+4\Big)\,\mathrm{Li}_3(x)+\Bigg(2\,L_x^2+\Big(6\,L_y-4\Big)\,L_x-2\,L_y+4\,\pi^2\Bigg)\,\mathrm{Li}_2(x)\\
&+\Big(18\,L_x\,L_y-4\,L_y^2\Big)\,\mathrm{Li}_2(y)+\frac{4}{3}\,L_x^4+\Big(-3\,L_y-\frac{8}{3}\Big)\,L_x^3\\
&+\Big(15\,L_y^2+L_y+\frac{1}{12}\,\pi^2-\frac{15}{4}\Big)\,L_x^2+\Big(-L_y^3-4\,L_y^2-2\,L_y\,\pi^2+\frac{11}{12}\,\pi^2+8\,\zeta_3+6\Big)\,L_x\\
&-\frac{1}{6}\,L_y^4+\frac{7}{3}\,L_y^3+\Big(\frac{7}{12}\,\pi^2-\frac{9}{4}\Big)\,L_y^2+\Big(\frac{3}{4}\,\pi^2-16\,\zeta_3+6\Big)\,L_y\\
&+\frac{1}{30}\,\pi^4-\frac{4}{3}\,\pi^2+4\,\zeta_3\Bigg]\,\Bigg[\frac{t^2-u^2}{s^2}\Bigg]+\Big[3\,L_x^2\Big]\,\frac{t^3}{s^2u}+\Big[3\,L_y^2\Big]\,\frac{u^3}{s^2t}\\
&+4\,\mathrm{Li}_3(y)+2\,\mathrm{Li}_3(x)+\Big(-2\,L_x+4\,L_y\Big)\,\mathrm{Li}_2(x)+\frac{3}{4}\,L_x^3+\Big(-\frac{7}{4}\,L_y-\frac{15}{4}\Big)\,L_x^2\\
&+\Big(\frac{5}{4}\,L_y^2-\frac{3}{2}\,L_y+\frac{5}{12}\,\pi^2-6\Big)\,L_x+\frac{7}{4}\,L_y^3+\frac{9}{4}\,L_y^2+\Big(-\frac{19}{12}\,\pi^2+6\Big)\,L_y\\
&+\pi^2-12\,\zeta_3
\end{aligned}
\tag{4.33}
$$

$$
D_s=\Bigg[\frac{2}{3}\,\mathrm{Li}_3(x)-\frac{2}{3}\,L_x\,\mathrm{Li}_2(x)-\frac{22}{9}\,L_s^2+\Big(-2\,L_x+\frac{2}{3}\,L_x^2+\frac{389}{54}\Big)\,L_s
$$

$$+\frac{2}{9}\,L_x^3+\left(-\frac{29}{18}-\frac{1}{3}\,L_y\right)L_x^2+\left(\frac{10}{9}\,\pi^2+\frac{11}{6}\right)L_x$$
$$+\left(-\frac{1}{12}\,\pi^2+\frac{25}{54}\right)L_y-\frac{455}{54}+\frac{41}{36}\,\pi^2-\frac{49}{18}\,\zeta_3\Bigg]\left[\frac{t^2+u^2}{s^2}\right]$$
$$+\left[\left(\frac{1}{3}\,L_x^2-\frac{1}{3}\,L_x\right)L_s+\frac{1}{9}\,L_x^3-\frac{13}{18}\,L_x^2+\left(\frac{4}{9}\,\pi^2+\frac{8}{9}\right)L_x-\frac{2}{9}\,\pi^2\right]\left[\frac{t^2-u^2}{s^2}\right]$$
$$+\frac{1}{3}\,L_x\,L_s-\frac{1}{6}\,L_x^2-\frac{8}{9}\,L_x+\frac{2}{9}\,\pi^2 \tag{4.34}$$

$$E_s=\Bigg[\frac{4}{3}\,\mathrm{Li}_3(y)-\frac{4}{3}\,\mathrm{Li}_3(x)+\left(\frac{4}{3}\,L_y+\frac{4}{3}\,L_x\right)\mathrm{Li}_2(x)-\frac{4}{9}\,L_x^3+\left(\frac{29}{9}+\frac{2}{3}\,L_y\right)L_x^2$$
$$+\left(4\,L_x-4\,L_y+\frac{4}{3}\,L_y^2+\frac{29}{6}-\frac{4}{3}\,L_x^2\right)L_s+\left(-\frac{223}{54}+\frac{2}{3}\,L_y^2-\frac{77}{36}\,\pi^2\right)L_x$$
$$+\frac{4}{9}\,L_y^3-\frac{29}{9}\,L_y^2+\left(\frac{223}{54}+\frac{23}{12}\,\pi^2\right)L_y-\frac{35}{18}\,\zeta_3-\frac{685}{81}-\frac{7}{36}\,\pi^2\Bigg]\left[\frac{t^2+u^2}{s^2}\right]$$
$$+\Bigg[\left(-\frac{2}{3}\,L_x^2+\frac{2}{3}\,L_x+\frac{2}{3}\,L_y-\frac{2}{3}\,L_y^2\right)L_s-\frac{2}{9}\,L_x^3+\frac{13}{9}\,L_x^2$$
$$+\left(-\frac{8}{9}\,\pi^2-\frac{16}{9}\right)L_x-\frac{2}{9}\,L_y^3+\frac{13}{9}\,L_y^2+\left(-\frac{8}{9}\,\pi^2-\frac{16}{9}\right)L_y+\frac{8}{9}\,\pi^2\Bigg]\left[\frac{t^2-u^2}{s^2}\right]$$
$$+\left(-\frac{2}{3}\,L_x+\frac{2}{3}\,L_y\right)L_s-\frac{16}{9}\,L_y-\frac{1}{3}\,L_y^2+\frac{16}{9}\,L_x+\frac{1}{3}\,L_x^2 \tag{4.35}$$

$$F_s=\left(-\frac{20}{27}\,L_s+\frac{50}{81}-\frac{2}{9}\,\pi^2+\frac{2}{9}\,L_s^2\right)\left[\frac{t^2+u^2}{s^2}\right] \tag{4.36}$$

We can check some of these results by comparing with the analytic expressions presented in Ref. [17] for the QED process $e^+e^-\to\mu^+\mu^-$. Taking the QED limit corresponds to setting $C_A=0$, $C_F=1$, $T_R=1$ as well as setting the cubic Casimir $C_3=(N^2-1)(N^2-2)/N^2=0$. This means that we can directly compare $E_s(\propto C_F T_R\,N_F)$ and $F_s(\propto T_R^2\,N_F^2)$ but *not* C_s which receives contributions from both C_3 and C_F^2. We see that (4.35) and (4.36) agree with Eqs. (2.38) and (2.39) of [17] respectively.

The other coefficients, A_s, B_s, C_s and D_s are new results.

4.2.2 The t-channel process $q+\bar{q}'\to q+\bar{q}'$

The t-channel process, $q+\bar{q}'\to q+\bar{q}'$ is fixed by $\mathcal{A}^8(t,s,u)$. We find that the finite two-loop contribution in the t-channel is given by Eq. (4.30) with

$$A_t=\Bigg[-2\,\mathrm{Li}_4(x)+\left(2\,L_x-\frac{11}{3}\right)\mathrm{Li}_3(x)+\left(\frac{11}{3}\,L_x-L_x^2+\frac{2}{3}\,\pi^2\right)\mathrm{Li}_2(x)$$

$$
\begin{aligned}
&+\frac{121}{18}\,L_s^2+\left(\frac{22}{9}\,L_x-\frac{11}{3}\,L_x^2-\frac{296}{27}\right)L_s+\frac{1}{4}\,L_x^4+\left(-\frac{14}{9}-\frac{1}{3}\,L_y\right)L_x^3\\
&+\left(-\frac{7}{6}\,\pi^2+\frac{20}{3}+\frac{11}{6}\,L_y\right)L_x^2+\left(\zeta_3-\frac{46}{9}+\frac{2}{3}\,L_y\,\pi^2-\frac{373}{72}\,\pi^2\right)L_x\\
&+\left(-\frac{409}{216}+\frac{11}{24}\,\pi^2-7\,\zeta_3\right)L_y+\frac{23213}{2592}-\frac{49}{9}\,\pi^2+\frac{197}{36}\,\zeta_3-\frac{1}{48}\,\pi^4\Bigg]\left[\frac{s^2+u^2}{t^2}\right]\\
&+\Bigg[-3\,\mathrm{Li}_4\left(\frac{x-1}{x}\right)-3\,\mathrm{Li}_4(y)-6\,\mathrm{Li}_4(x)+\left(5\,L_x-\frac{7}{2}\right)\mathrm{Li}_3(x)\\
&+3\,L_x\,\mathrm{Li}_3(y)+\left(-\frac{1}{2}\,\pi^2-\frac{1}{2}\,L_x^2+\frac{7}{2}\,L_x\right)\mathrm{Li}_2(x)+\left(-\frac{11}{6}\,L_x-\frac{11}{6}\,L_x^2\right)L_s\\
&-\frac{1}{6}\,L_x^4+\left(-\frac{19}{18}+L_y\right)L_x^3+\left(-\frac{1}{2}\,\pi^2+\frac{55}{18}+\frac{7}{4}\,L_y\right)L_x^2\\
&+\left(-\frac{1}{2}\,L_y\,\pi^2-\frac{20}{9}\,\pi^2+\frac{32}{9}-2\,\zeta_3\right)L_x-\frac{19}{36}\,\pi^2+\frac{29}{120}\,\pi^4+2\,\zeta_3\Bigg]\left[\frac{s^2-u^2}{t^2}\right]\\
&+\left[3\,L_x^2\right]\frac{s^3}{t^2u}+3\,\mathrm{Li}_4\left(\frac{x-1}{x}\right)+3\,\mathrm{Li}_4(y)+3\,\mathrm{Li}_4(x)+\left(-3\,L_x-\frac{5}{2}\right)\mathrm{Li}_3(x)\\
&-3\,L_x\,\mathrm{Li}_3(y)+\left(\frac{1}{2}\,\pi^2+\frac{5}{2}\,L_x\right)\mathrm{Li}_2(x)+\frac{11}{6}\,L_x\,L_s+\frac{1}{4}\,L_x^4+\left(-L_y-\frac{3}{4}\right)L_x^3\\
&+\left(\frac{5}{4}\,L_y+2\right)L_x^2+\left(\frac{1}{2}\,L_y\,\pi^2-\frac{32}{9}+\frac{7}{6}\,\pi^2\right)L_x-\frac{5}{24}\,\pi^4+\frac{55}{36}\,\pi^2+4\,\zeta_3 \qquad (4.37)
\end{aligned}
$$

$$
\begin{aligned}
B_t=&\Bigg[6\,\mathrm{Li}_4(x)+\left(-6\,L_x+\frac{44}{3}\right)\mathrm{Li}_3(x)+\left(\frac{22}{3}\,L_y-\frac{44}{3}\,L_x-2\,\pi^2+3\,L_x^2\right)\mathrm{Li}_2(x)\\
&+\frac{22}{3}\,\mathrm{Li}_3(y)+\left(-\frac{88}{3}-\frac{22}{3}\,L_y^2+22\,L_y-\frac{22}{3}\,\pi^2+\frac{44}{3}\,L_x\,L_y\right)L_s-L_y\,L_x^3\\
&+\left(-L_y^3+\frac{29}{3}\,L_y^2+\left(-\frac{187}{9}-\frac{7}{3}\,\pi^2\right)L_y-\frac{52}{3}+\frac{25}{3}\,\pi^2\right)L_x\\
&+\left(4\,\pi^2+2\,L_y^2+3-\frac{16}{3}\,L_y\right)L_x^2+\frac{1}{4}\,L_y^4-\frac{71}{18}\,L_y^3+\left(\frac{5}{6}\,\pi^2+\frac{689}{36}\right)L_y^2\\
&+\left(-\frac{407}{72}\,\pi^2-\zeta_3-\frac{275}{27}\right)L_y+\frac{30659}{648}-\frac{77}{720}\,\pi^4-\frac{707}{36}\,\zeta_3+\frac{183}{8}\,\pi^2\Bigg]\left[\frac{s^2+u^2}{t^2}\right]\\
&+\Bigg[-12\,\mathrm{Li}_4\left(\frac{x-1}{x}\right)-8\,\mathrm{Li}_4(y)-3\,\mathrm{Li}_4(x)+\left(-14\,L_y+10\,L_x-\frac{5}{2}\right)\mathrm{Li}_3(x)\\
&+\left(-8-2\,L_y+2\,L_x\right)\mathrm{Li}_3(y)+\left(-\frac{5}{2}\,L_x^2+\left(4\,L_y+\frac{5}{2}\right)L_x-8\,L_y-\frac{8}{3}\,\pi^2\right)\mathrm{Li}_2(x)\\
&+\left(\frac{22}{3}\,L_x^2+\left(-\frac{22}{3}\,L_y+\frac{22}{3}\right)L_x+\frac{11}{3}\,\pi^2-\frac{11}{3}\,L_y+\frac{11}{3}\,L_y^2\right)L_s-\frac{5}{12}\,L_x^4\\
&+\left(\frac{73}{18}+L_y\right)L_x^3+\left(-\frac{41}{12}\,L_y-\frac{3}{2}\,L_y^2-\frac{193}{18}+\frac{11}{6}\,\pi^2\right)L_x^2
\end{aligned}
$$

$$
\begin{aligned}
&+\Bigg(\frac{1}{3}\,L_y^3 - 7\,L_y^2 + \Bigg(\frac{7}{6}\,\pi^2 + \frac{295}{18}\Bigg)\,L_y - \frac{101}{9} - 8\,\zeta_3 + \frac{92}{9}\,\pi^2\Bigg)\,L_x - \frac{1}{6}\,L_y^4 + \frac{17}{9}\,L_y^3 \\
&+\Bigg(- \frac{5}{12}\,\pi^2 - \frac{361}{36}\Bigg)\,L_y^2 + \Bigg(\frac{64}{9} + \frac{167}{36}\,\pi^2 + 8\,\zeta_3\Bigg)\,L_y - \zeta_3 + \frac{29}{90}\,\pi^4 - \frac{91}{12}\,\pi^2\Bigg]\,\Bigg[\frac{s^2-u^2}{t^2}\Bigg] \\
&-\Bigg[7\,L_x^2\Bigg]\,\frac{s^3}{t^2u} + \Bigg[5\,L_y^2 - 10\,L_x\,L_y + 5\,\pi^2 + 5\,L_x^2\Bigg]\,\frac{u^3}{t^2 s} - 12\,\mathrm{Li}_4\Bigg(\frac{x-1}{x}\Bigg) \\
&-12\,\mathrm{Li}_4(y) - 12\,\mathrm{Li}_4(x) + \Bigg(12\,L_x - 6\,L_y + \frac{21}{2}\Bigg)\,\mathrm{Li}_3(x) + \Bigg(6 + 6\,L_x\Bigg)\,\mathrm{Li}_3(y) \\
&+\Bigg(- \frac{21}{2}\,L_x - 2\,\pi^2 + 6\,L_y\Bigg)\,\mathrm{Li}_2(x) - \frac{11}{3}\,L_s\,L_y - \frac{1}{2}\,L_x^4 + \Bigg(- \frac{1}{6} + 3\,L_y\Bigg)\,L_x^3 \\
&+\Bigg(\frac{5}{2} + \frac{1}{2}\,\pi^2 - \frac{3}{4}\,L_y - \frac{3}{2}\,L_y^2\Bigg)\,L_x^2 + \Bigg(- \frac{16}{3}\,L_y - 3 + 2\,L_y^2 - \frac{29}{6}\,\pi^2 - 6\,\zeta_3\Bigg)\,L_x \\
&+\frac{1}{4}\,L_y^3 + \frac{7}{12}\,L_y^2 + \Bigg(- 2\,\pi^2 + 6\,\zeta_3 + \frac{64}{9}\Bigg)\,L_y + \frac{5}{12}\,\pi^2 + \frac{13}{20}\,\pi^4 - \zeta_3
\end{aligned}
\tag{4.38}
$$

$$
\begin{aligned}
C_t = &\Bigg[16\,\mathrm{Li}_4\Bigg(\frac{x-1}{x}\Bigg) + \Bigg(16\,L_y - 8\,L_x\Bigg)\,\mathrm{Li}_3(x) + \Bigg(- 16\,L_x + 16\,L_y\Bigg)\,\mathrm{Li}_3(y) \\
&-8\,\mathrm{Li}_4(x) + \Bigg(4\,L_x^2 + 8\,L_y^2 + \frac{16}{3}\,\pi^2 - 16\,L_x\,L_y\Bigg)\,\mathrm{Li}_2(x) + \frac{2}{3}\,L_x^4 - \frac{4}{3}\,L_y\,L_x^3 \\
&+\Bigg(3 - 5\,L_y^2 - \frac{5}{3}\,\pi^2\Bigg)\,L_x^2 + \Bigg(5\,L_y^3 + 9\,L_y^2 + \Bigg(\frac{7}{3}\,\pi^2 - 19\Bigg)\,L_y + 16\,\zeta_3 - 9\,\pi^2\Bigg)\,L_x \\
&+\frac{1}{12}\,L_y^4 - \frac{9}{2}\,L_y^3 + \Bigg(\frac{65}{4} - \frac{19}{6}\,\pi^2\Bigg)\,L_y^2 + \Bigg(- \frac{189}{8} - 10\,\zeta_3 - 5\,\pi^2\Bigg)\,L_y \\
&+\pi^4 - \frac{15}{2}\,\zeta_3 + \frac{511}{32} + \frac{95}{24}\,\pi^2\Bigg]\,\Bigg[\frac{s^2+u^2}{t^2}\Bigg] \\
&+\Bigg[12\,\mathrm{Li}_4\Bigg(\frac{x-1}{x}\Bigg) + 24\,\mathrm{Li}_4(y) + 24\,\mathrm{Li}_4(x) + \Bigg(- 24\,L_x + 8\,L_y + 6\Bigg)\,\mathrm{Li}_3(x) \\
&+\Bigg(6\,L_x^2 + \Bigg(- 6 - 4\,L_y\Bigg)\,L_x - 4\,L_y^2 + 4\,\pi^2 + 2\,L_y\Bigg)\,\mathrm{Li}_2(x) \\
&+\Bigg(- 10\,L_y - 8\,L_x + 2\Bigg)\,\mathrm{Li}_3(y) + \frac{5}{6}\,L_x^4 + \Bigg(2\,L_y - 2\,L_y^2 - \frac{7}{3}\,\pi^2 - 6\Bigg)\,L_x^2 \\
&+\Bigg(- \frac{2}{3}\,L_y + \frac{2}{3}\Bigg)\,L_x^3 + \Bigg(- \frac{7}{3}\,L_y^3 - 3\,L_y^2 + \Bigg(\frac{9}{2} + \frac{19}{6}\,\pi^2\Bigg)\,L_y + 16\,\zeta_3 - \frac{19}{3}\,\pi^2 - 12\Bigg)\,L_x \\
&-\frac{1}{6}\,L_y^4 + \frac{7}{3}\,L_y^3 + \Bigg(\frac{1}{4}\,\pi^2 - \frac{9}{4}\Bigg)\,L_y^2 + \Bigg(\frac{13}{12}\,\pi^2 + 6 - 6\,\zeta_3\Bigg)\,L_y \\
&-\frac{43}{12}\,\pi^2 - \frac{7}{4}\,\pi^4 + 2\,\zeta_3\Bigg]\,\Bigg[\frac{s^2-u^2}{t^2}\Bigg] + \Bigg[3\,L_x^2\Bigg]\,\frac{s^3}{t^2u} + \Bigg[3\,\pi^2 - 6\,L_x\,L_y + 3\,L_y^2 + 3\,L_x^2\Bigg]\,\frac{u^3}{t^2s} \\
&-2\,\mathrm{Li}_3(x) - 4\,\mathrm{Li}_3(y) + \Bigg(2\,L_x - 4\,L_y\Bigg)\,\mathrm{Li}_2(x) + \Bigg(- 3 + 2\,L_y\Bigg)\,L_x^2
\end{aligned}
$$

$$+\left(\pi^2 - 3\,L_y - \frac{13}{2}\,L_y^2\right)L_x + \frac{7}{4}\,L_y^3 + \frac{9}{4}\,L_y^2 + \left(6 + \frac{7}{2}\,\pi^2\right)L_y + \frac{7}{4}\,\pi^2 - 8\,\zeta_3 \qquad (4.39)$$

$$\begin{aligned}
D_t = &\left[\frac{2}{3}\,\mathrm{Li}_3(x) - \frac{2}{3}\,L_x\,\mathrm{Li}_2(x) - \frac{22}{9}\,L_s^2 + \left(-\frac{26}{9}\,L_x + \frac{2}{3}\,L_x^2 + \frac{389}{54}\right)L_s\right.\\
&+\frac{5}{9}\,L_x^3 + \left(-\frac{37}{18} - \frac{1}{3}\,L_y\right)L_x^2 + \left(\frac{265}{54} + \frac{11}{36}\,\pi^2\right)L_x + \left(\frac{25}{54} - \frac{1}{12}\,\pi^2\right)L_y\\
&\left.-\frac{49}{18}\,\zeta_3 - \frac{455}{54} + \frac{25}{36}\,\pi^2\right]\left[\frac{s^2+u^2}{t^2}\right]\\
&+\left[\left(\frac{1}{3}\,L_x^2 + \frac{1}{3}\,L_x\right)L_s + \frac{2}{9}\,L_x^3 - \frac{7}{18}\,L_x^2 + \left(-\frac{8}{9} + \frac{2}{9}\,\pi^2\right)L_x + \frac{1}{9}\,\pi^2\right]\left[\frac{s^2-u^2}{t^2}\right]\\
&-\frac{1}{3}\,L_x\,L_s - \frac{1}{9}\,\pi^2 + \frac{8}{9}\,L_x - \frac{1}{2}\,L_x^2 \qquad (4.40)
\end{aligned}$$

$$\begin{aligned}
E_t = &\left[-\frac{8}{3}\,\mathrm{Li}_3(x) - \frac{4}{3}\,\mathrm{Li}_3(y) + \left(-\frac{4}{3}\,L_y + \frac{8}{3}\,L_x\right)\mathrm{Li}_2(x) - \frac{2}{3}\,L_x^2\,L_y\right.\\
&+\left(-4\,L_y + \frac{4}{3}\,\pi^2 + \frac{4}{3}\,L_y^2 + \frac{29}{6} - \frac{8}{3}\,L_x\,L_y\right)L_s + \left(\frac{29}{6} + \frac{22}{9}\,L_y - \frac{2}{3}\,L_y^2 + \frac{2}{3}\,\pi^2\right)L_x\\
&\left.+\frac{4}{9}\,L_y^3 - \frac{29}{9}\,L_y^2 + \left(\frac{223}{54} + \frac{37}{36}\,\pi^2\right)L_y - \frac{41}{12}\,\pi^2 - \frac{685}{81} - \frac{11}{18}\,\zeta_3\right]\left[\frac{s^2+u^2}{t^2}\right]\\
&+\left[\left(-\frac{4}{3}\,L_x^2 + \left(\frac{4}{3}\,L_y - \frac{4}{3}\right)L_x - \frac{2}{3}\,\pi^2 + \frac{2}{3}\,L_y - \frac{2}{3}\,L_y^2\right)L_s - \frac{8}{9}\,L_x^3\right.\\
&+\left(\frac{14}{9} + \frac{2}{3}\,L_y\right)L_x^2 + \left(-\frac{20}{9}\,L_y - \frac{8}{9}\,\pi^2 + \frac{32}{9}\right)L_x - \frac{2}{9}\,L_y^3 + \frac{13}{9}\,L_y^2\\
&\left.+\left(-\frac{16}{9} - \frac{2}{9}\,\pi^2\right)L_y + \pi^2\right]\left[\frac{s^2-u^2}{t^2}\right]\\
&+\frac{4}{3}\,L_x\,L_y + \frac{2}{3}\,L_s\,L_y - \frac{1}{3}\,L_y^2 - \frac{1}{3}\,\pi^2 - \frac{16}{9}\,L_y \qquad (4.41)
\end{aligned}$$

$$F_t = \left[\frac{2}{9}\,L_s^2 + \left(\frac{4}{9}\,L_x - \frac{20}{27}\right)L_s + \frac{2}{9}\,L_x^2 - \frac{20}{27}\,L_x + \frac{50}{81}\right]\left[\frac{s^2+u^2}{t^2}\right] \qquad (4.42)$$

4.2.3 The u-channel process $q + q' \to q + q'$

The u-channel process, $q + q' \to q + q'$ is determined by $A^8(u,t,s)$. We find that the finite two-loop contribution in the u-channel is given by Eq. (4.30) with

$$\begin{aligned}
A_u = &\left[-2\,\mathrm{Li}_4\left(\frac{x-1}{x}\right) + \left(2\,L_x + \frac{11}{3} - 2\,L_y\right)\mathrm{Li}_3(x) + \left(2\,L_x + \frac{11}{3} - 2\,L_y\right)\mathrm{Li}_3(y)\right.\\
&+\left(-L_x^2 + \left(-\frac{11}{3} + 2\,L_y\right)L_x - \frac{1}{3}\,\pi^2 + \frac{11}{3}\,L_y - L_y^2\right)\mathrm{Li}_2(x) + \frac{121}{18}\,L_s^2
\end{aligned}$$

$$
\begin{aligned}
&+\biggl(-\frac{11}{3}L_x^2+\Bigl(11+\frac{22}{3}L_y\Bigr)L_x-\frac{11}{3}\pi^2-\frac{296}{27}+\frac{22}{9}L_y-\frac{11}{3}L_y^2\biggr)L_s+\frac{1}{12}L_x^4\\
&+\Bigl(-\frac{49}{18}-\frac{2}{3}L_y\Bigr)L_x^3+\Bigl(2L_y^2+\frac{197}{18}+\frac{8}{3}L_y\Bigr)L_x^2+\biggl(-\frac{5}{3}L_y^3\\
&+\frac{17}{6}L_y^2+\Bigl(-\frac{2}{3}\pi^2-\frac{98}{9}\Bigr)L_y+4\zeta_3-\frac{95}{24}-\frac{31}{9}\pi^2\biggr)L_x+\frac{1}{4}L_y^4\\
&-\frac{14}{9}L_y^3+\Bigl(\frac{1}{2}\pi^2+\frac{20}{3}\Bigr)L_y^2+\Bigl(-\frac{46}{9}-\frac{25}{8}\pi^2+3\zeta_3\Bigr)L_y+\frac{17}{144}\pi^4+\frac{65}{36}\zeta_3\\
&+\frac{11}{2}\pi^2+\frac{23213}{2592}\biggr)\left[\frac{t^2+s^2}{u^2}\right]+\biggl(-6\,\mathrm{Li}_4\Bigl(\frac{x-1}{x}\Bigr)+3\,\mathrm{Li}_4(x)+3\,\mathrm{Li}_4(y)\\
&+\Bigl(2L_x-2L_y+\frac{7}{2}\Bigr)\mathrm{Li}_3(x)+\Bigl(-5L_y+\frac{7}{2}+5L_x\Bigr)\mathrm{Li}_3(y)\\
&+\Bigl(-\frac{1}{2}L_x^2+\Bigl(-\frac{7}{2}+L_y\Bigr)L_x-\pi^2+\frac{7}{2}L_y-\frac{1}{2}L_y^2\Bigr)\mathrm{Li}_2(x)\\
&+\biggl(-\frac{11}{6}L_x^2+\Bigl(\frac{11}{6}+\frac{11}{3}L_y\Bigr)L_x-\frac{11}{6}\pi^2-\frac{11}{6}L_y-\frac{11}{6}L_y^2\biggr)L_s-\frac{1}{8}L_x^4\\
&+\Bigl(\frac{1}{2}L_y-\frac{49}{36}\Bigr)L_x^3+\Bigl(-\frac{1}{4}\pi^2+\frac{1}{2}L_y+\frac{3}{4}L_y^2+\frac{44}{9}\Bigr)L_x^2+\biggl(-\frac{5}{6}L_y^3\\
&+\frac{37}{12}L_y^2+\Bigl(-\frac{5}{6}\pi^2-\frac{143}{18}\Bigr)L_y-\frac{32}{9}-3\zeta_3-\frac{67}{36}\pi^2\biggr)L_x-\frac{1}{24}L_y^4-\frac{19}{18}L_y^3\\
&+\Bigl(-\frac{5}{12}\pi^2+\frac{55}{18}\Bigr)L_y^2+\Bigl(-\frac{83}{36}\pi^2+3\zeta_3+\frac{32}{9}\Bigr)L_y-\frac{3}{2}\zeta_3-\frac{7}{120}\pi^4+\frac{157}{36}\pi^2\biggr]\left[\frac{t^2-s^2}{u^2}\right]\\
&+\Bigl[-6L_xL_y+3L_y^2+3\pi^2+3L_x^2\Bigr]\frac{t^3}{u^2s}\\
&+3\,\mathrm{Li}_4\Bigl(\frac{x-1}{x}\Bigr)-3\,\mathrm{Li}_4(x)-3\,\mathrm{Li}_4(y)+\frac{5}{2}\mathrm{Li}_3(x)+\Bigl(\frac{5}{2}-3L_x+3L_y\Bigr)\mathrm{Li}_3(y)\\
&+\Bigl(\frac{5}{2}L_y-\frac{5}{2}L_x+\frac{1}{2}\pi^2\Bigr)\mathrm{Li}_2(x)+\Bigl(\frac{11}{6}L_y-\frac{11}{6}L_x\Bigr)L_s+\frac{1}{8}L_x^4\\
&+\Bigl(\frac{1}{3}-\frac{1}{2}L_y\Bigr)L_x^3+\Bigl(\frac{1}{6}+\frac{1}{4}\pi^2-\frac{9}{4}L_y\Bigr)L_x^2+\biggl(\frac{7}{2}L_y^2+\Bigl(-\frac{13}{6}+\frac{1}{2}\pi^2\Bigr)L_y\\
&+\frac{32}{9}+3\zeta_3-\frac{1}{6}\pi^2\biggr)L_x+\frac{1}{8}L_y^4-\frac{3}{4}L_y^3+\Bigl(2+\frac{1}{2}\pi^2\Bigr)L_y^2\\
&+\Bigl(-3\zeta_3-\frac{32}{9}-\frac{3}{2}\pi^2\Bigr)L_y+\frac{3}{2}\zeta_3+\frac{61}{36}\pi^2+\frac{11}{120}\pi^4
\end{aligned}
\tag{4.43}
$$

$$
\begin{aligned}
B_u=&\biggl[6\,\mathrm{Li}_4\Bigl(\frac{x-1}{x}\Bigr)+\Bigl(-\frac{22}{3}+6L_y-6L_x\Bigr)\mathrm{Li}_3(x)+\Bigl(-\frac{44}{3}-6L_x+6L_y\Bigr)\mathrm{Li}_3(y)\\
&+\Bigl(3L_x^2+\Bigl(-6L_y+\frac{22}{3}\Bigr)L_x+3L_y^2-\frac{44}{3}L_y+\pi^2\Bigr)\mathrm{Li}_2(x)+\Bigl(\frac{22}{3}L_x^2
\end{aligned}
$$

$$
\begin{aligned}
&+\Big(-22-\frac{44}{3}\,L_y\Big)\,L_x-\frac{88}{3}+\frac{22}{3}\,\pi^2\Big)\,L_s-\frac{1}{4}\,L_x^4+\Big(2\,L_y+\frac{125}{18}\Big)\,L_x^3\\
&+\Big(-\frac{11}{2}\,L_y^2-\frac{743}{36}-\frac{25}{3}\,L_y+\frac{1}{2}\,\pi^2\Big)\,L_x^2+\Big(4\,L_y^3-\frac{28}{3}\,L_y^2+\Big(\frac{133}{9}+\frac{7}{3}\,\pi^2\Big)\,L_y\\
&+\frac{535}{72}\,\pi^2+7\,\zeta_3-\frac{49}{27}\Big)\,L_x+\Big(-\frac{5}{2}\,\pi^2+3\Big)\,L_y^2+\Big(-\frac{52}{3}+\frac{1}{9}\,\pi^2-6\,\zeta_3\Big)\,L_y\\
&-\frac{1217}{72}\,\pi^2+\frac{30659}{648}-\frac{437}{720}\,\pi^4-\frac{179}{36}\,\zeta_3\Big)\,\Big[\frac{t^2+s^2}{u^2}\Big]+\Big(-3\,\mathrm{Li}_4\Big(\frac{x-1}{x}\Big)+8\,\mathrm{Li}_4(x)\\
&+12\,\mathrm{Li}_4(y)+\Big(-4\,L_x-8\,L_y-\frac{11}{2}\Big)\,\mathrm{Li}_3(x)+\Big(\frac{5}{2}-10\,L_y-4\,L_x\Big)\,\mathrm{Li}_3(y)\\
&+\Big(\frac{3}{2}\,L_x^2+\Big(\frac{11}{2}+L_y\Big)\,L_x-\frac{5}{2}\,L_y^2+\frac{5}{2}\,L_y-\frac{7}{6}\,\pi^2\Big)\,\mathrm{Li}_2(x)+\Big(\frac{11}{3}\,L_x^2+\Big(-\frac{11}{3}\\
&-\frac{22}{3}\,L_y\Big)\,L_x+\frac{11}{3}\,\pi^2+\frac{22}{3}\,L_y+\frac{22}{3}\,L_y^2\Big)\,L_s-\frac{1}{2}\,L_x^4+\Big(\frac{131}{36}+\frac{7}{3}\,L_y\Big)\,L_x^3\\
&+\Big(-\frac{289}{36}-\frac{3}{4}\,\pi^2-\frac{15}{4}\,L_y^2-\frac{7}{2}\,L_y\Big)\,L_x^2+\Big(-\frac{11}{6}\,L_y^3+\frac{13}{12}\,L_y^2+\Big(\frac{223}{18}+\frac{17}{6}\,\pi^2\Big)\,L_y\\
&+\frac{73}{18}\,\pi^2+\frac{37}{9}+4\,\zeta_3\Big)\,L_x+\frac{1}{12}\,L_y^4+\frac{73}{18}\,L_y^3+\Big(\frac{3}{4}\,\pi^2-\frac{193}{18}\Big)\,L_y^2+\Big(\frac{191}{36}\,\pi^2\\
&+2\,\zeta_3-\frac{101}{9}\Big)\,L_y-\frac{67}{12}\,\pi^2-\frac{7}{2}\,\zeta_3-\frac{61}{90}\,\pi^4\Big]\,\Big[\frac{t^2-s^2}{u^2}\Big]\\
&+\Big[-7\,\pi^2-7\,L_x^2-7\,L_y^2+14\,L_x\,L_y\Big]\,\frac{t^3}{u^2s}+5\,\frac{s^3}{u^2t}\,L_y^2-12\,\mathrm{Li}_4\Big(\frac{x-1}{x}\Big)+12\,\mathrm{Li}_4(x)\\
&+12\,\mathrm{Li}_4(y)+\Big(-\frac{9}{2}-6\,L_y\Big)\,\mathrm{Li}_3(x)+\Big(6\,L_x-\frac{21}{2}-12\,L_y\Big)\,\mathrm{Li}_3(y)\\
&+\Big(-\frac{21}{2}\,L_y+\frac{9}{2}\,L_x-2\,\pi^2\Big)\,\mathrm{Li}_2(x)+\frac{11}{3}\,L_x\,L_s-\frac{1}{2}\,L_x^4+\Big(-\frac{5}{6}+2\,L_y\Big)\,L_x^3\\
&+\Big(-\frac{3}{2}\,L_y^2+\frac{17}{12}+\frac{9}{2}\,L_y-\pi^2\Big)\,L_x^2+\Big(\frac{1}{12}\,\pi^2-\frac{37}{4}\,L_y^2-6\,\zeta_3+\frac{1}{3}\,L_y-\frac{37}{9}-L_y^3\Big)\,L_x\\
&-\frac{1}{6}\,L_y^3+\Big(\frac{5}{2}-\frac{3}{2}\,\pi^2\Big)\,L_y^2+\Big(\frac{65}{12}\,\pi^2+6\,\zeta_3-3\Big)\,L_y+\frac{5}{4}\,\pi^2-\frac{11}{20}\,\pi^4+\frac{19}{2}\,\zeta_3
\end{aligned}
\tag{4.44}
$$

$$
\begin{aligned}
C_u=&\Big[-8\,\mathrm{Li}_4\Big(\frac{x-1}{x}\Big)-16\,\mathrm{Li}_4(y)+\Big(8\,L_x-8\,L_y\Big)\,\mathrm{Li}_3(x)+\Big(8\,L_x+8\,L_y\Big)\,\mathrm{Li}_3(y)\\
&+\Big(8\,L_x\,L_y+4\,L_y^2-4\,L_x^2-\frac{20}{3}\,\pi^2\Big)\,\mathrm{Li}_2(x)+\frac{1}{12}\,L_x^4+\Big(-\frac{5}{3}\,L_y-\frac{9}{2}\Big)\,L_x^3\\
&+\Big(9\,L_y+\frac{1}{4}+5\,L_y^2-\frac{11}{6}\,\pi^2\Big)\,L_x^2+\Big(\frac{8}{3}\,L_y^3+\Big(13-3\,\pi^2\Big)\,L_y-4\,\pi^2+\frac{189}{8}-14\,\zeta_3\Big)\,L_x\\
&+\Big(3-\frac{11}{3}\,\pi^2\Big)\,L_y^2+\Big(-9\,\pi^2+8\,\zeta_3\Big)\,L_y+\frac{9}{5}\,\pi^4-\frac{289}{24}\,\pi^2-\frac{15}{2}\,\zeta_3+\frac{511}{32}\Big]\,\Big[\frac{t^2+s^2}{u^2}\Big]
\end{aligned}
$$

$$
\begin{aligned}
&+\Bigg[24\,\mathrm{Li}_4\left(\frac{x-1}{x}\right)-24\,\mathrm{Li}_4(x)-12\,\mathrm{Li}_4(y)+\Bigg(-4+16\,L_y+2\,L_x\Bigg)\,\mathrm{Li}_3(x)\\
&+\Bigg(-6-16\,L_x+24\,L_y\Bigg)\,\mathrm{Li}_3(y)+\Bigg(-2\,L_x^2+\Bigg(-8\,L_y+4\Bigg)\,L_x-6\,L_y\\
&+6\,\pi^2+6\,L_y^2\Bigg)\,\mathrm{Li}_2(x)+\frac{4}{3}\,L_x^4+\Bigg(-\frac{19}{3}\,L_y-\frac{8}{3}\Bigg)\,L_x^3+\Bigg(7\,L_y+2\,L_y^2-\frac{15}{4}\\
&+\frac{25}{12}\,\pi^2\Bigg)\,L_x^2+\Bigg(\frac{10}{3}\,L_y^3-10\,L_y^2+\Bigg(\frac{15}{2}-\frac{1}{2}\,\pi^2\Bigg)\,L_y-\frac{13}{12}\,\pi^2+6\,\zeta_3+6\Bigg)\,L_x+\frac{1}{3}\,L_y^4\\
&+\frac{2}{3}\,L_y^3+\Bigg(\frac{5}{3}\,\pi^2-6\Bigg)\,L_y^2+\Bigg(\frac{20}{3}\,\pi^2-8\,\zeta_3-12\Bigg)\,L_y-\frac{61}{12}\,\pi^2+\frac{21}{20}\,\pi^4+8\,\zeta_3\Bigg]\,\left[\frac{t^2-s^2}{u^2}\right]\\
&+\Bigg[-6\,L_x\,L_y+3\,L_y^2+3\,\pi^2+3\,L_x^2\Bigg]\,\frac{t^3}{u^2 s}\\
&+3\,\frac{s^3}{u^2 t}\,L_y^2-2\,\mathrm{Li}_3(x)+2\,\mathrm{Li}_3(y)+\Bigg(2\,L_y+2\,L_x\Bigg)\,\mathrm{Li}_2(x)+\frac{3}{4}\,L_x^3\\
&+\Bigg(-\frac{1}{2}\,L_y-\frac{15}{4}\Bigg)\,L_x^2+\Bigg(9\,L_y+\frac{7}{6}\,\pi^2-6\Bigg)\,L_x+\frac{8}{3}\,L_y\,\pi^2-\frac{17}{4}\,\pi^2-3\,L_y^2-10\,\zeta_3
\end{aligned}
\tag{4.45}
$$

$$
\begin{aligned}
D_u=&\Bigg[-\frac{2}{3}\,\mathrm{Li}_3(x)-\frac{2}{3}\,\mathrm{Li}_3(y)+\Bigg(\frac{2}{3}\,L_x-\frac{2}{3}\,L_y\Bigg)\,\mathrm{Li}_2(x)-\frac{22}{9}\,L_s^2\\
&+\Bigg(\frac{2}{3}\,L_x^2+\Bigg(-2-\frac{4}{3}\,L_y\Bigg)\,L_x+\frac{2}{3}\,L_y^2-\frac{26}{9}\,L_y+\frac{389}{54}+\frac{2}{3}\,\pi^2\Bigg)\,L_s\\
&+\frac{2}{9}\,L_x^3+\Bigg(\frac{1}{3}\,L_y-\frac{29}{18}\Bigg)\,L_x^2+\Bigg(\frac{4}{9}\,\pi^2-\frac{4}{3}\,L_y^2+\frac{11}{9}\,L_y+\frac{11}{6}\Bigg)\,L_x\\
&+\frac{5}{9}\,L_y^3-\frac{37}{18}\,L_y^2+\Bigg(\frac{3}{4}\,\pi^2+\frac{265}{54}\Bigg)\,L_y-\frac{455}{54}-\frac{11}{12}\,\pi^2-\frac{37}{18}\,\zeta_3\Bigg]\,\left[\frac{t^2+s^2}{u^2}\right]\\
&+\Bigg[\Bigg(\frac{1}{3}\,L_x^2+\Bigg(-\frac{1}{3}-\frac{2}{3}\,L_y\Bigg)\,L_x+\frac{1}{3}\,L_y+\frac{1}{3}\,\pi^2+\frac{1}{3}\,L_y^2\Bigg)\,L_s\\
&+\frac{1}{9}\,L_x^3-\frac{13}{18}\,L_x^2+\Bigg(-\frac{1}{3}\,L_y^2+\frac{1}{9}\,\pi^2+\frac{8}{9}+\frac{10}{9}\,L_y\Bigg)\,L_x+\frac{2}{9}\,L_y^3\\
&-\frac{7}{18}\,L_y^2+\Bigg(-\frac{8}{9}+\frac{2}{9}\,\pi^2\Bigg)\,L_y-\frac{11}{18}\,\pi^2\Bigg]\,\left[\frac{t^2-s^2}{u^2}\right]\\
&+\Bigg(\frac{1}{3}\,L_x-\frac{1}{3}\,L_y\Bigg)\,L_s-\frac{1}{6}\,L_x^2+\Bigg(-\frac{8}{9}+\frac{2}{3}\,L_y\Bigg)\,L_x-\frac{5}{18}\,\pi^2+\frac{8}{9}\,L_y-\frac{1}{2}\,L_y^2
\end{aligned}
\tag{4.46}
$$

$$
E_u=\Bigg[\frac{4}{3}\,\mathrm{Li}_3(x)+\frac{8}{3}\,\mathrm{Li}_3(y)+\Bigg(-\frac{4}{3}\,L_x+\frac{8}{3}\,L_y\Bigg)\,\mathrm{Li}_2(x)
$$

$$
\begin{aligned}
&+\Bigg(-\frac{4}{3}\,L_x^2+\bigg(\frac{8}{3}\,L_y+4\bigg)\,L_x-\frac{4}{3}\,\pi^2+\frac{29}{6}\bigg)\,L_s-\frac{4}{9}\,L_x^3+\bigg(\frac{29}{9}-\frac{2}{3}\,L_y\bigg)\,L_x^2\\
&+\bigg(\frac{10}{3}\,L_y^2-\frac{223}{54}-\frac{29}{36}\,\pi^2-\frac{22}{9}\,L_y\bigg)\,L_x+\bigg(-\frac{10}{9}\,\pi^2+\frac{29}{6}\bigg)\,L_y\\
&-\frac{685}{81}-\frac{59}{18}\,\zeta_3+\frac{109}{36}\,\pi^2\Bigg]\left[\frac{t^2+s^2}{u^2}\right]\\
&+\Bigg[\bigg(-\frac{2}{3}\,L_x^2+\bigg(\frac{2}{3}+\frac{4}{3}\,L_y\bigg)\,L_x-\frac{4}{3}\,L_y-\frac{2}{3}\,\pi^2-\frac{4}{3}\,L_y^2\bigg)\,L_s-\frac{2}{9}\,L_x^3+\frac{13}{9}\,L_x^2\\
&+\bigg(\frac{2}{3}\,L_y^2-\frac{20}{9}\,L_y-\frac{2}{9}\,\pi^2-\frac{16}{9}\bigg)\,L_x-\frac{8}{9}\,L_y^3+\frac{14}{9}\,L_y^2+\bigg(\frac{32}{9}-\frac{8}{9}\,\pi^2\bigg)\,L_y+\pi^2\Bigg]\left[\frac{t^2-s^2}{u^2}\right]\\
&-\frac{2}{3}\,L_x\,L_s+\frac{1}{3}\,L_x^2+\bigg(-\frac{4}{3}\,L_y+\frac{16}{9}\bigg)\,L_x+\frac{1}{3}\,\pi^2 \qquad (4.47)
\end{aligned}
$$

$$
F_u=\left[\frac{2}{9}\,L_s^2+\bigg(\frac{4}{9}\,L_y-\frac{20}{27}\bigg)\,L_s+\frac{2}{9}\,L_y^2-\frac{20}{27}\,L_y+\frac{50}{81}\right]\left[\frac{t^2+s^2}{u^2}\right] \qquad (4.48)
$$

5. Summary

In this paper we presented the two-loop QCD corrections to the scattering of two distinct massless quarks. Throughout, we have used conventional dimensional regularisation and the $\overline{\rm MS}$ scheme to compute the interference of the tree and two-loop graphs summed over spins and colours. The pole structure is given in Eq. (4.12) while expressions for the finite parts are given for each of the s-, t- and u-channels in Secs. 4.2.1, 4.2.2 and 4.2.3 respectively.

The leading infrared singularity is $\mathcal{O}\left(1/\epsilon^4\right)$ and it is a very strong check on the reliability of our calculation that the pole structure obtained by computing the Feynman diagrams agrees with that anticipated by Catani through to $\mathcal{O}\left(1/\epsilon\right)$. For the finite N_F/N and N_F^2 contributions, we agree with prior QED calculations.

These results form a crucial part of the next-to-next-to-leading order predictions for jet cross sections in hadron-hadron collisions. However, they are only a part of the whole and must be combined with the tree-level $2 \to 4$, the one-loop $2 \to 3$ as well as the square of the one-loop $2 \to 2$ processes to yield physical cross sections. For the most part, the matrix elements themselves are available in the literature. Each of the contributions is divergent in the infrared limit and a systematic procedure for analytically canceling the infrared divergences needs to be established for semi-inclusive jet cross sections. Here again, some progress has been made by examining the limits of tree-level matrix elements when two particles are unresolved [31, 32] and the soft and collinear limits of one-loop amplitudes [33, 34]. The somewhat simpler case of $e^+e^- \to$ photon + jet at next-to-leading order which involves the triple collinear limit of tree-level matrix elements as well as the collinear limit of one-loop amplitudes has already been studied [35] and indicates that the technical problems are not insurmountable. Another technical difficulty will be to isolate the initial state singularities and correctly absorb them into the parton density functions at next-to-next-to-leading order. Recent progress towards the three-loop splitting functions [36, 37, 38] together with accurate parameterisations in x-space [39, 40] suggest that the factorisation can be achieved. Modifications to the global fits to provide parton density functions appropriate for next-to-next-to-leading order calculations are already underway [41]. In summary, we are therefore confident that these problems will soon be overcome thereby enabling the analytic cancellation of the infrared divergences and the construction of numerical programs to provide next-to-next-to-leading order QCD estimates of observable scattering cross sections.

Acknowledgements

We thank Adrian Signer and Bas Tausk for helpful suggestions and Stefano Catani for clarifying the content of Ref. [18].

C.A. acknowledges the financial support of the Greek Government and M.E.T. acknowledges financial support from CONACyT and the CVCP. C.O. thanks S. Catani for useful discussions. We gratefully acknowledge the support of the British Council and German Academic Exchange Service under ARC project 1050. This work was supported in part by the EU Fourth Framework Programme 'Training and Mobility of Researchers', Network 'Quantum Chromodynamics and the Deep Structure of Elementary Particles', contract FMRX-CT98-0194 (DG-12-MIHT).

References

[1] F. Abe et al., CDF Collaboration, Phys. Rev. Lett. **77** (1996) 438 [hep-ex/9601008].

[2] B. Abbott et al., D0 Collaboration, Phys. Rev. Lett. **82** (1999) 2451 [hep-ex/9807018].

[3] S.D. Ellis, Z. Kunzst and D.E. Soper, Phys. Rev. Lett. **69** (1992) 3615 [hep-ph/9208249].

[4] W.T. Giele, E.W.N. Glover and D.A. Kosower, Phys.Rev. **D52** (1995) 1486 [hep-ph/9412338].

[5] Z. Bern, L. Dixon, D.A. Kosower, Phys. Rev. Lett **70** (1993) 2677 [hep-ph/9302280].

[6] Z. Bern, L. Dixon and D.A. Kosower, Nucl. Phys. **B437** (1995) 259 [hep-ph/9409393].

[7] Z. Kunszt, A. Signer and Z. Trócsányi, *Phys. Lett* **B336** (1994) 529 [hep-ph/9405386].

[8] J.F. Gunion and J. Kalinowski, Phys. Rev. **D34** (1986) 2119;
S.J. Parke and T.R. Taylor, Nucl. Phys. **B269** (1986) 410;
F.A. Berends and W.T. Giele, Nucl. Phys. **B294** (1987) 700;
M. Mangano, S.J. Parke and Z. Xu, Nucl. Phys. **B298** (1988) 653.

[9] Z. Kunszt, Nucl. Phys. **B271** (1986) 333;
S.J. Parke and T.J. Taylor, Phys. Rev. **D35** (1987) 313.

[10] J.F. Gunion and Z. Kunszt, Phys. Lett. **159B** (1985) 167.

[11] J.F. Gunion and Z. Kunszt, Phys. Lett. **176B** (1986) 163.

[12] V.A. Smirnov, Phys. Lett. **B460** (1999) 397 [hep-ph/9905323].

[13] J.B. Tausk, Phys. Lett. **B469** (1999) 225 [hep-ph/9909506].

[14] V.A. Smirnov and O.L. Veretin, Nucl. Phys. **B566** (2000) 469 [hep-ph/9907385].

[15] C. Anastasiou, T. Gehrmann, C. Oleari, E. Remiddi and J.B. Tausk, Nucl. Phys. **B580** (2000) 577 [hep-ph/0003261].

[16] Z. Bern, L. Dixon and D.A. Kosower, JHEP **0001** (2000) 027 [hep-ph/0001001].

[17] Z. Bern, L. Dixon and A. Ghinculov, hep-ph/0010075.

[18] S. Catani, Phys. Lett. **B427** (1998) 161 [hep-ph/9802439].

[19] R.K. Ellis and J.C. Sexton, Nucl. Phys. **B269** (1986) 445.

[20] R.J. Gonsalves, Phys. Rev. **D28** (1983) 1542;
G. Kramer and B. Lampe, J. Math. Phys. **28** (1987) 945.

[21] C. Anastasiou, E.W.N. Glover and C. Oleari, Nucl. Phys. **B572** (2000) 307 [hep-ph/9907494].

[22] C. Anastasiou, E.W.N. Glover and C. Oleari, Nucl. Phys. **B575** (2000) 416, Erratum-ibid. **B585** (2000) 763 [hep-ph/9912251].

[23] E.W.N. Glover and M.E. Tejeda-Yeomans, Nucl. Phys. Proc. Suppl. **89** (2000) 196 [hep-ph/0010031].

[24] T. Gehrmann and E. Remiddi, Nucl. Phys. Proc. Suppl. **89** (2000) 2512 [hep-ph/0005232].

[25] C. Anastasiou, J.B. Tausk and M.E. Tejeda-Yeomans, Nucl. Phys. Proc. Suppl. **89** (2000) 262 [hep-ph/0005328].

[26] O.V. Tarasov, Phys. Rev. **D54**(1996) 6479 [hep-th/9606018], Nucl. Phys. **B502** (1997) 455 [hep-ph/9703319].

[27] K.G. Chetyrkin, A.L. Kataev and F.V. Tkachov, Nucl. Phys. **B174** (1980) 345 ;
K.G. Chetyrkin and F.V. Tkachov, Nucl. Phys. **B192** (1981) 159.

[28] T. Gehrmann and E. Remiddi, Nucl. Phys. **B580** (2000) 485 [hep-ph/9912329].

[29] P. Nogueira, J.Comput.Phys. **105** (1993) 279.

[30] K.S. Kölbig, J.A. Mignaco and E. Remiddi, *B.I.T.* **10** (1970) 38.

[31] J.M. Campbell and E.W.N. Glover, Nucl. Phys. **B527** (1998) 264 [hep-ph/9710255]; S. Catani and M. Grazzini, Phys. Lett. **446B** (1999) 143 [hep-ph/9810389], Nucl. Phys. **B570** (2000) 287 [hep-ph/9908523].

[32] F.A. Berends and W.T. Giele, Nucl. Phys. **B313** (1989) 595;
S. Catani, in Proceedings of the workshop on *New Techniques for Calculating Higher Order QCD Corrections*, report ETH-TH/93-01, Zurich (1992).

[33] Z. Bern, V. Del Duca and C.R. Schmidt, Phys. Lett. **445B** (1998) 168 [hep-ph/9810409];
Z. Bern, V. Del Duca, W.B. Kilgore and C.R. Schmidt, Phys. Rev. **D60** (1999) 116001 [hep-ph/9903516];
S. Catani and M. Grazzini, hep-ph/0007142.

[34] Z. Bern, L. Dixon, D.C. Dunbar and D.A. Kosower, Nucl. Phys. **B425** (1994) 217 [hep-ph/9403226];
D.A. Kosower, Nucl. Phys. **B552** (1999) 319;
D.A. Kosower and P. Uwer, Nucl. Phys. **B563** (1999) 477 [hep-ph/9903515].

[35] A. Gehrmann-De Ridder and E.W.N. Glover, Nucl. Phys. **B517** (1998) 269 [hep-ph/9707224].

[36] S.A. Larin, T. van Ritbergen, and J.A.M. Vermaseren, Nucl. Phys. **B427** (1994) 41;
S.A. Larin, P. Nogueira, T. van Ritbergen, and J.A.M. Vermaseren, Nucl. Phys. **B492** (1997) 338 [hep-ph/9605317].

[37] A. Retey and J.A.M. Vermaseren, `hep-ph/0007294`.

[38] J. A. Gracey, Phys. Lett. **B322** (1994) 141 [hep-ph/9401214].

[39] W.L. van Neerven and A. Vogt, Nucl. Phys. **B568** (2000) 263 [hep-ph/9907472]; hep-ph/0006154.

[40] W.L. van Neerven and A. Vogt, Phys. Lett. **B490** (2000) 111 [hep-ph/0007362].

[41] A.D. Martin, R.G. Roberts, W.J. Stirling and R.S. Thorne, hep-ph/0007099.